

Non-overlap Average Treatment Effect Bounds

Herbert P. Susmann*, Alec McClean*, and Iván Díaz

Division of Biostatistics, Department of Population Health, New York University Grossman School of Medicine, New York, USA
 *equal contribution.

Abstract

The average treatment effect (ATE), the mean difference in potential outcomes under treatment and control, is a canonical causal effect. *Overlap*, which says that all subjects have non-zero probability of either treatment status, is necessary to identify and estimate the ATE. When overlap fails, the standard solution is to change the estimand, and target a trimmed effect in a subpopulation satisfying overlap; however, this no longer addresses the original goal of estimating the ATE. When the outcome is bounded, we demonstrate that this compromise is unnecessary. We derive *non-overlap bounds*: partial identification bounds on the ATE that do not require overlap. They are the sum of a trimmed effect within the overlap subpopulation and worst-case bounds on the ATE in the non-overlap subpopulation. Non-overlap bounds have width proportional to the size of the non-overlap subpopulation, making them informative when overlap violations are limited — a common scenario in practice. Since the bounds are non-smooth functionals, we derive smooth approximations of them that contain the ATE but can be estimated using debiased estimators leveraging semiparametric efficiency theory. Specifically, we propose a Targeted Minimum Loss-Based estimator that is \sqrt{n} -consistent and asymptotically normal under nonparametric assumptions on the propensity score and outcome regression. We then show how to obtain a uniformly valid confidence set across all trimming and smoothing parameters with the multiplier bootstrap. This allows researchers to consider many parameters, choose the tightest confidence interval, and still attain valid coverage. We demonstrate via simulations that non-overlap bound estimators can detect non-zero ATEs with higher power than traditional doubly-robust point estimators. We illustrate our method by estimating the ATE of right heart catheterization on mortality.

Keywords: causal inference, average treatment effect, positivity violations, targeted minimum loss-based estimation

1 Introduction

A paradigmatic target of counterfactual causal inference is the *average treatment effect* (ATE), defined as the population difference in potential outcomes under assignment to treatment vs control (Rosenbaum and Rubin, 1983; Robins, 1986). Estimating the ATE requires three foundational assumptions. The first assumption, *consistency* (also known as the *stable unit treatment value assumption*, or *SUTVA*) requires that each unit's observed outcome is equal to their potential

outcome for their observed treatment status. The second assumption, *conditional exchangeability* (also known as *no unmeasured confounding* and *selection on observables*), requires that all common causes of the treatment and outcome are measured. The third assumption, *overlap* (also known as *positivity* or *common support*), requires that all units have a propensity score (the probability of receiving treatment given covariates) that is neither zero nor one. Structural violations of overlap occur when there exists a subpopulation with propensity score that is zero or one, preventing identification of the ATE. In other cases, units may have a small yet non-zero probability of receiving either treatment status. In finite samples, such practical violations of the overlap assumption manifest as strata of covariates with few or zero observed treated (or control) units (Zhu et al., 2021). When overlap holds structurally, but is not satisfied in practice, then the ATE is identified, yet statistical estimators may exhibit poor finite-sample performance (Petersen et al., 2012).

A common strategy when faced with practical positivity violations is to abandon the ATE in favor of an alternative estimand that either does not require overlap or requires a weaker form of overlap (Petersen et al., 2012). Moving to effects defined by alternative counterfactual interventions is one way to avoid the requirement of overlap; for example, effects defined in terms of incremental propensity score interventions (Kennedy, 2019). Alternatively, the target population can be changed to a subpopulation in which overlap is satisfied, referred to as the *overlap* or *equipoise* population (Greifer and Stuart, 2023). Methods for estimating the treatment effect within the overlap subpopulation include propensity score trimming (Crump et al., 2009; McClean and Díaz, 2025) and cardinality matching (Visconti and Zubizarreta, 2018). Overlap balancing weights (Li et al., 2018a) target the overlap population by smoothly down-weighting observations which do not satisfy overlap. The shortcoming of pivoting to an alternative estimand is that the original object of inquiry, the ATE, is abandoned (Rizk, 2025). Furthermore, popular alternative estimands are typically less interpretable than the ATE. For example, propensity score trimming targets the overlap subpopulation, which can be difficult to interpret particularly in high dimensions; indeed, methods for characterizing the overlap subpopulation is itself an active area of research (Traskin and Small, 2011; Karavani et al., 2019; Wolf et al., 2021).

An alternative set of approaches to addressing non-identifiability emphasizes the derivation of *partial identification bounds* that bracket the counterfactual parameter of interest under a weaker set of assumptions (Richardson et al., 2014). For the ATE, Manski (1990) and Robins (1989) independently derived bounds (sometimes referred to as *Manski bounds*) for bounded outcomes that require neither conditional exchangeability nor overlap. However, their bounds are non-informative in the sense that they always include zero, and never rule out the possibility of a null treatment effect. Sharper bounds were subsequently derived under alternative conditions, such as monotonicity in treatment or response (Manski, 1997; Manski and Pepper, 2000). Focusing on the conditional exchangeability assumption, there has been significant interest in the development of ATE bounds in the presence of unmeasured confounding under various sensitivity models (Cornfield et al., 1959; Schlesselman, 1978; Rosenbaum and Rubin, 1983; Lin et al., 1998; Nabi et al., 2024; VanderWeele and Arah, 2011; Díaz and van der Laan, 2013; Bonvini and Kennedy, 2022). For non-overlap, relatively fewer developments have been proposed; Lee and Weidner (2021b) propose bounds on the ATE based on an assumption that also relaxes consistency; under the standard consistency assumption, their bounds reduce to the non-informative Manski bounds. Closer to our work is Zivich et al. (2024b), who propose a method for transporting causal effects between source and target populations lacking overlap with respect to a single continuous covariate. Supposing researchers can characterize the overlap and non-overlap populations in terms of a single covariate, their method then combines traditional causal transport estimators in the overlap subpopulation with counterfactual outcome imputation via a pre-specified mathematical model in the non-overlap

subpopulation.

In this work, we propose a novel approach for the identification and estimation of the partial identification bounds for the ATE that do not require overlap and do not require a priori knowledge of the overlap population. The core contributions, spanning identification, estimation, and demonstration of finite-sample performance, are described below.

Contribution 1 We propose novel partial identification bounds for the ATE that are identified only assuming consistency, conditional exchangeability and boundedness of the outcome, but not overlap. These bounds, which we refer to as *non-overlap bounds*, combine a point estimate of the average treatment effect within a subpopulation satisfying overlap with an analysis of the “worst-case” treatment effect among the complementary non-overlap subpopulation, using a definition of overlap in terms of a propensity score threshold. Our derivation follows directly from the analysis in Manski (1990) – we essentially take their derivation one step further by dividing the population into overlap and non-overlap subpopulations. However, as opposed to Manski bounds, the non-overlap bounds we propose are informative in the sense that they exclude zero and achieve sign-identification of the ATE in realistic scenarios. Specifically, the non-overlap bounds are informative whenever the proportion of the population in the non-overlap subpopulation is smaller than the magnitude of the treatment effect in the overlap population.

Contribution 2 Turning to estimation, our second contribution is to propose an estimator for the bounds that achieves \sqrt{n} -rate convergence in realistic nonparametric models. While the non-overlap bounds are irregular, in that they have a non-smooth relationship with the propensity score, we derive a carefully chosen smooth approximation of the non-overlap bounds that can be analyzed using tools from semiparametric efficiency theory (Begin et al., 1983; Bickel et al., 1997; van der Vaart, 1998), allowing estimation at \sqrt{n} -rates under nonparametric assumptions via a Targeted Minimum Loss-Based Estimation approach and valid inference for the ATE (van der Laan and Rubin, 2006; van der Laan and Rose, 2011). However, this approach introduces a practical challenge for researchers. A priori, it is unclear which propensity score threshold or smoothing parameter researchers ought to choose to obtain the narrowest confidence interval for the ATE. To solve this problem, we use the multiplier bootstrap to construct a uniform confidence set for the ATE over a grid of propensity score thresholds and smoothing parameters. Crucially, this allows researchers to choose the narrowest confidence interval in the set and still obtain appropriate coverage of the ATE. Therefore, a null hypothesis of null treatment effect may be rejected if the narrowest confidence interval for the ATE excludes zero.

Contribution 3 Finally, our third contribution is to demonstrate in finite-sample scenarios the utility of non-overlap bounds in comparison to traditional ATE estimators. In a simulation study designed to exhibit practical violations of the overlap assumption, we compare non-overlap bounds to a doubly-robust one-step estimator of the ATE, and find the non-overlap bounds are able to achieve higher power, shorter uncertainty width, and better empirical coverage. We further illustrate the non-overlap bounds in an application to estimating the ATE of right heart catheterization on mortality (Murphy and Cluff, 1990; Connors et al., 1996). This case study has been used previously to test methods for causal inference under non-overlap, allowing us to compare our estimated bounds against results of other methods applied to the same dataset (Hirano and Imbens, 2001; Crump et al., 2009; Traskin and Small, 2011; Rosenbaum, 2012; Li et al., 2018a; Rothe, 2017; Lee and Weidner, 2021b; Ma et al., 2024). Both the simulation and data application demonstrate that even with large

non-overlap subpopulations it is possible to conduct statistically valid inference on the ATE, and it is not necessary to abandon the ATE in favor of alternative (e.g., weighted or trimmed) estimands.

The remainder of the manuscript proceeds as follows. In Section 2, we introduce notation and formally define the ATE in terms of the potential outcomes framework for causal inference. Non-overlap bounds for the ATE, and their smooth approximations, are derived in Section 3. An estimator based on TMLE and a multiplier bootstrap based method for uniform confidence sets is given in Section 4. A simulation study is presented in Section 5, and an illustrative application studying the effect of right heart catheterization on mortality in Section 6. We conclude with a discussion in Section 7.

2 Background

Suppose we observe n i.i.d. copies Z_1, \dots, Z_n of the generic random variable $Z \in \mathcal{Z}$ drawn from the law \mathbb{P} falling in the nonparametric statistical model \mathcal{P} ; that is, $Z \sim \mathbb{P} \in \mathcal{P}$. We let $Z = (X, A, Y)$, where X is a vector of covariates, $A \in \{0, 1\}$ a binary treatment indicator, and Y is, without loss of generality, a bounded outcome in $[0, 1]$. Let Y^0 and Y^1 be the potential outcomes under counterfactual treatment assignments $A = 0$ and $A = 1$, respectively (Imbens, 2004). We define the *propensity score* as $\pi \equiv \pi(X) \equiv \mathbb{P}(A = 1 | X)$ and the *outcome model* as $\mu_a \equiv \mu_a(X) \equiv \mathbb{E}(Y | A = a, X)$ for $a \in \{0, 1\}$, where \mathbb{E} denotes expectation with respect to \mathbb{P} . We let $\eta = \{\pi, \mu_0, \mu_1\}$ be the set gathering the nuisance functions. Throughout this paper, unless necessary for clarity, we will omit covariate arguments so that, e.g., $\mathbb{P}(\pi \leq c) \equiv \mathbb{P}\{\pi(X) \leq c\}$.

The Average Treatment Effect (ATE) is defined in terms of potential outcomes as $\psi = \mathbb{E}(Y^1 - Y^0)$. Point-identifying the ATE in terms of the observed data requires the following assumptions:

Assumption 1 (Consistency). $Y = Y(A)$.

Assumption 2 (No unmeasured confounding). $Y^a \perp\!\!\!\perp A | X$.

Assumption 3 (Overlap). *It holds \mathbb{P} -almost everywhere that $0 < \pi < 1$.*

Under Assumptions 1, 2, and 3, the ATE is identified by the *g-formula* (Hernán and Robins, 2020):

$$\psi = \mathbb{E}\{\mathbb{E}(Y | A = 1, X) - \mathbb{E}(Y | A = 0, X)\} \equiv \mathbb{E}\{\mu_1(X) - \mu_0(X)\}.$$

Remark 1 (Structural vs practical overlap violations). Crucially, the g-formula identification result requires overlap (Assumption 3). *Structural* Overlap violations occur when $\mathbb{P}\{\pi(X) = 0\} > 0$ or $\mathbb{P}\{\pi(X) = 1\} > 0$. In this case, the g-formula does not hold, because $\mathbb{E}\{\mu_1(X) - \mu_0(X)\}$ is not defined. *Practical* overlap violations occur when there exists some X such that $\pi(X) \in (0, 1)$, but where $\pi(X) \approx 0$ or $\pi(X) \approx 1$. This has two important consequences. First, in a specific sample, observations within strata X will be unbalanced, in the sense that most or all subjects will take treatment $A = 1$ (if $\pi(X) \approx 1$) or control $A = 0$ (if $\pi(X) \approx 0$). As a result, although practical overlap violations do not prevent identification, they can have a profound effect on the finite-sample statistical performance of estimators, which will typically have very large variance.

Notation The indicator function is denoted $\mathbb{I}(a)$, equaling one when the predicate a is true and zero otherwise. We denote convergence in distribution by \rightsquigarrow and convergence in probability by \xrightarrow{P} . For a function $z \mapsto f(z)$, we write $\|f\| = \sqrt{\int f(z)^2 d\mathbb{P}(z)}$ to denote the $L_2(\mathbb{P})$ -norm, $\mathbb{E}(f) = \int f(z) d\mathbb{P}$ the expectation of f with respect to \mathbb{P} , $\mathbb{P}(A) = \mathbb{E}\{\mathbb{I}(A)\}$ to denote the probability of A , where A is

some event, and $\mathbb{P}_n(f) = n^{-1} \sum_{i=1}^n f(Z_i)$ the empirical mean of f with respect to Z_1, \dots, Z_n . For simplicity, we may write $\mathbb{E} \equiv \mathbb{E}_{\mathbb{P}}$. We write $a \lesssim b$ when $a \leq Cb$ for a constant C . For $N \geq 1$, we write $[N] = \{1, \dots, N\}$.

3 Bounding the Population Average Treatment Effect

In this section, we derive and identify informative bounds on the ATE when the overlap assumption is violated.

3.1 Informative non-overlap bounds

When the overlap assumption (Assumption 3) does not hold, the ATE is not identifiable. However, when the potential outcomes are bounded it is possible to derive identifiable bounds for the ATE, as we demonstrate in the following result.

Proposition 1 (Non-overlap bounds). *Let $c \in [0, \frac{1}{2}]$ denote a propensity score trimming threshold. Under Assumptions 1 and 2,*

$$\mathbb{E}(Y^1 - Y^0) \in [L(c), U(c)]. \quad (1)$$

where

$$\begin{aligned} L(c) &= \psi(c) - \mathbb{P}(\pi \geq 1 - c), \\ U(c) &= \psi(c) + \mathbb{P}(\pi \leq c), \text{ and} \\ \psi(c) &= \mathbb{E}\{\mu_1(X)\mathbb{I}(\pi > c) - \mu_0(X)\mathbb{I}(\pi < 1 - c)\} \end{aligned}$$

Proof. The argument proceeds in three steps. First,

$$\begin{aligned} \mathbb{E}(Y^1) &= \mathbb{E}\{Y^1\mathbb{I}(\pi > c)\} + \mathbb{E}(Y^1 | \pi \leq c)\mathbb{P}(\pi \leq c) \text{ and} \\ \mathbb{E}(Y^0) &= \mathbb{E}\{Y^0\mathbb{I}(\pi < 1 - c)\} + \mathbb{E}(Y^0 | \pi \geq 1 - c)\mathbb{P}(\pi \geq 1 - c). \end{aligned}$$

Therefore, the ATE satisfies

$$\mathbb{E}(Y^1 - Y^0) = \mathbb{E}\{Y^1\mathbb{I}(\pi > c) - Y^0\mathbb{I}(\pi < 1 - c)\} + \mathbb{E}(Y^1 | \pi \leq c)\mathbb{P}(\pi \leq c) - \mathbb{E}(Y^0 | \pi \geq 1 - c)\mathbb{P}(\pi \geq 1 - c).$$

Second, the bounds in the result then follow by imposing the bounds $\{Y^0, Y^1\} \in [0, 1]$ on $\mathbb{E}(Y^1 | \pi \leq c)$ and $\mathbb{E}(Y^0 | \pi \geq 1 - c)$. Finally, overlap is not required to identify $\mathbb{E}\{Y^1\mathbb{I}(\pi > c) - Y^0\mathbb{I}(\pi < 1 - c)\}$, and therefore the identification of the central term in the bounds, $\psi(c)$, follows under only Assumptions 1 and 2 by standard arguments. \square

The derivation of Proposition 1 is straightforward, yet is to our knowledge novel. The result is an interesting extension to the canonical worst-case identification bounds under unmeasured confounding (Manski, 1990; Robins, 1989). In essence, one splits the population into two parts: one where a treatment effect is identifiable because overlap is satisfied, and one where worst-case bounds must be applied.

However, unlike worst-case bounds under unmeasured confounding, it is plausible that our bounds are informative, in the sense they exclude zero and allow for sign-identification of the ATE. An important negative result in the sensitivity analysis literature states that without further assumptions, worst-case bounds under unmeasured confounding are uninformative, and must

include include zero (Manski, 1990). Crucially, however, because we focus on overlap violations rather than unmeasured confounders, *non-overlap bounds can exclude zero* in reasonable scenarios. Simple analysis shows that the bounds will be informative when either $\psi(c) > \mathbb{P}(\pi \geq 1 - c)$ or $\psi(c) < -\mathbb{P}(\pi \leq c)$. That is, the bounds will be informative when the size of the overlap-violating set is smaller than the magnitude of the identifiable treatment effect. This is a reasonable scenario we envisage can often occur in practice, whenever the scale of overlap violations is minor compared to the identifiable effect.

3.2 Smooth valid bounds

The bounds in eq. (1) are non-smooth because they depend on indicator functions of the propensity score: $\mathbb{I}(\pi > c)$, $\mathbb{I}(\pi < 1 - c)$, etc. The non-differentiability of these indicator functions poses challenges for estimation under nonparametric assumptions. Although \sqrt{n} -rate estimation and valid inference may be possible with a well-specified parametric model for the propensity score or with specific nonparametric assumptions, general guarantees are unavailable. We address this issue by constructing smooth approximations of the lower and upper bounds, which yields pathwise differentiable parameters that can be estimated at \sqrt{n} -rates under general nonparametric assumptions. Crucially, we show that these smooth bounds *contain the non-smooth bounds*, and therefore, although the smooth bounds may be wider, they still always contain the ATE and facilitate valid statistical inference for it.

The core of our approach is to replace the indicator functions implicit in eq. (1) with smooth approximations. We construct two smooth approximations. First, we construct $s_l(\cdot, c, \gamma) : [0, 1] \rightarrow [0, 1]$ as an approximation of $\mathbb{I}(\pi < c)$ (“l” for “ π less than c ”) and $s_g(\cdot, c, \gamma) : [0, 1] \rightarrow [0, 1]$ as an approximation of $\mathbb{I}(\pi > c)$ (“g” for “ π greater than c ”), where $\gamma > 0$ is a smoothing parameter. We provide details on these approximations subsequently. Given these functions, we define the smooth approximation of $\psi(c)$ as

$$\psi_s(c, \gamma) = \mathbb{E}\{\mu_1(X)s_g(\pi, c, \gamma) - \mu_0(X)s_l(\pi, 1 - c, \gamma)\}.$$

We also approximate the additional offset terms in the bounds of eq. (1). We approximate $\mathbb{P}(\pi \geq 1 - c) = 1 - \mathbb{P}(\pi < 1 - c)$ by $1 - \mathbb{E}\{s_l(\pi, 1 - c, \gamma)\}$ and $\mathbb{P}(\pi \leq c) = 1 - \mathbb{P}(\pi > c)$ by $1 - \mathbb{E}\{s_g(\pi, c, \gamma)\}$. From these, we construct smooth approximations of the bounds in eq. (1):

$$L_s(c, \gamma) = \psi_s(c, \gamma) - \left[1 - \mathbb{E}\{s_l(\pi, 1 - c, \gamma)\}\right] \text{ and} \quad (2)$$

$$U_s(c, \gamma) = \psi_s(c, \gamma) + \left[1 - \mathbb{E}\{s_g(\pi, c, \gamma)\}\right], \quad (3)$$

To guarantee the resulting smooth non-overlap bounds contain the ATE we must construct the smooth approximation functions to satisfy the following property.

Property 1. $s_l(x, c, \gamma) \leq \mathbb{I}(x < c)$ and $s_g(x, c, \gamma) \leq \mathbb{I}(x > c)$.

Property 1 requires that the approximations bound the respective indicator functions *from below*. Not all smooth approximations satisfy this property, but it is not difficult to construct functions

that do. For example:

$$s_l(x, c, \gamma) = \begin{cases} 1, & x \leq c - \gamma, \\ 0, & x \geq c, \\ 1 - \exp \left[1 + \frac{1}{\{(x-c)/\gamma\}^2 - 1} \right], & \text{otherwise, and} \end{cases} \quad (4)$$

$$s_g(x, c, \gamma) = \begin{cases} 1, & x \geq c + \gamma, \\ 0, & x \leq c, \\ 1 - \exp \left[1 + \frac{1}{\{(x-c)/\gamma\}^2 - 1} \right], & \text{otherwise.} \end{cases}$$

We use s_l and s_g as in (4) for the rest of the manuscript whenever a specific smooth approximation is needed. Figure 1 illustrates s_l and s_g for several decreasing choices of γ . As γ decreases, the smooth approximation gets closer to the relevant indicator function.

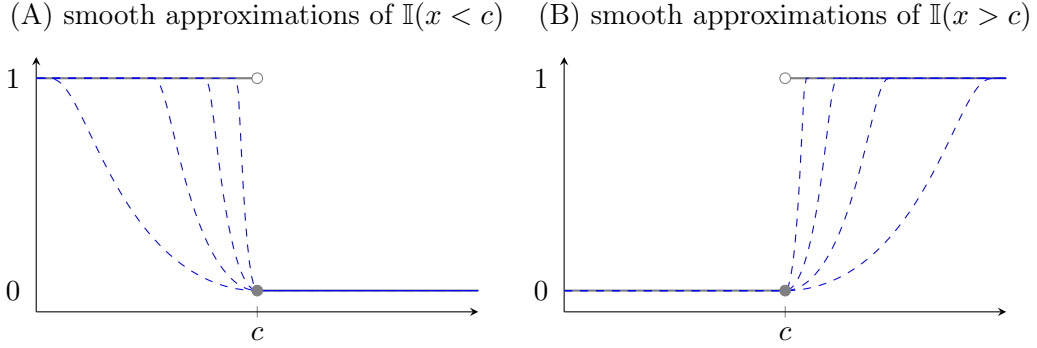


Figure 1: Example smooth approximations $s_l(x, c, \gamma)$ (A) and $s_g(x, c, \gamma)$ (B) as defined in (4) with smoothness $\gamma \in \{1, 0.5, 0.25, 0.1\}$.

The next result shows that if the smooth approximation functions satisfy Property 1 then they yield smooth bounds on the ATE.

Proposition 2 (Smooth non-overlap bounds). *Under the conditions of Proposition 1, suppose $s_l(x, c, \gamma)$ and $s_g(x, c, \gamma)$ satisfy Property 1. Then,*

$$\mathbb{E}(Y^1 - Y^0) \in [L_s(c, \gamma), U_s(c, \gamma)],$$

where $L_s(c, \gamma)$ and $U_s(c, \gamma)$ are defined in (2) and (3), respectively.

Proof. By Proposition 1, $\mathbb{E}(Y^1 - Y^0) \in [L(c), U(c)]$. Therefore, it is only necessary to show $L(c) \geq L_s(c, \gamma)$ and $U(c) \leq U_s(c, \gamma)$. Notice first that the smooth approximation error $\psi(c) - \psi_s(c, \gamma)$ satisfies

$$\psi(c) - \psi_s(c, \gamma) = \mathbb{E}[\mu_1(X)\{\mathbb{I}(\pi > c) - s_g(\pi, c, \gamma)\} - \mu_0(X)\{\mathbb{I}(\pi < 1 - c) - s_l(\pi, 1 - c, \gamma)\}].$$

The boundedness of the outcome and Property 1 imply

$$\mathbb{E}\{s_l(\pi, 1 - c, \gamma)\} - \mathbb{P}(\pi < 1 - c) \leq \psi(c) - \psi_s(c, \gamma) \leq \mathbb{P}(\pi > c) - \mathbb{E}\{s_g(\pi, c, \gamma)\}. \quad (5)$$

Applying these inequalities yields the result. For the lower bound,

$$\begin{aligned}
L_s(c) &= \psi(c) - \mathbb{P}(\pi \geq 1 - c) \\
&= \psi_s(c, \gamma) - \mathbb{P}(\pi \geq 1 - c) + \psi(c) - \psi_s(c, \gamma) \\
&\geq \psi_s(c, \gamma) - \mathbb{P}(\pi \geq 1 - c) + \mathbb{E}\{s_l(\pi, 1 - c, \gamma)\} - \mathbb{P}(\pi < 1 - c) \\
&= \psi_s(c, \gamma) - \left[1 - \mathbb{E}\{s_l(\pi, 1 - c, \gamma)\}\right] \equiv L_s(c, \gamma).
\end{aligned}$$

For the upper bound,

$$\begin{aligned}
U(c) &= \psi(c) + \mathbb{P}(\pi \leq c) \\
&= \psi_s(c, \gamma) + \mathbb{P}(\pi \leq c) + \psi(c) - \psi_s(c, \gamma) \\
&\leq \psi_s(c, \gamma) + \mathbb{P}(\pi \leq c) + \mathbb{P}(\pi > c) - \mathbb{E}\{s_g(\pi, c, \gamma)\} \\
&= \psi_s(c, \gamma) + \left[1 - \mathbb{E}\{s_g(\pi, c, \gamma)\}\right] \equiv U_s(c, \gamma).
\end{aligned}$$

□

Proposition 2 establishes the key guarantee, that the smooth bounds $L_s(c, \gamma)$ and $U_s(c, \gamma)$ contain the ATE while requiring only that the approximation functions satisfy Property 1—a condition easily ensured by construction. The proof illustrates why Property 1 is essential: it ensures that the smooth approximation error $\psi_s(c) - \psi(c)$ has the correct sign. Without this property, inequality (5) could fail, potentially yielding bounds that exclude the ATE.

This approach builds naturally on existing work with smooth approximations for non-smooth functionals, though two key distinctions merit attention (van der Laan and Luedtke, 2014). First, in standard point identification settings, the smooth approximation error typically lacks clear structure—it may be positive or negative without pattern. Consequently, an estimator targeting the smooth approximation does not implicitly target the original non-smooth parameter in any specific way. Instead, researchers must employ data-adaptive smoothing techniques that ensure the approximation error vanishes as sample size grows, thereby enabling valid inference for the non-smooth functional (Whitehouse et al., 2025).

Our partial identification framework sidesteps this complication entirely. Because our smooth bounds contain the non-smooth bounds by construction, we preserve valid ATE inference even when using fixed smoothing parameters. This guarantee—that smooth bounds maintain validity—has appeared previously with smooth instrumental variable bounds (Levis et al., 2025). However, our setting makes the smooth bounds more practically essential. While Levis et al. (2025) develop smooth bounds, they also achieve \sqrt{n} -rates for estimating non-smooth bounds under mild margin conditions. In their context, targeting non-smooth bounds directly remains both feasible and preferable from a practical standpoint. By contrast, achieving comparable rates for our non-smooth bounds would require substantially stronger assumptions, making the smooth approximation approach not merely convenient but practically necessary.

The practical implementation involves balancing smooth approximation error against statistical estimation error. Smaller values of γ yield bounds closer to the non-smooth target but increase the error of the resulting estimators. However, this tradeoff is often favorable in finite samples: we can typically choose γ such that statistical error dominates approximation error, yielding bounds that are both practically useful and statistically efficient. Furthermore, our proposed inference framework (developed in Section 4) allows practitioners to optimize over multiple (c, γ) combinations while preserving valid coverage for the ATE.

3.3 Efficiency theory

In this section, we derive the efficient influence function for the smooth bounds, which we will use in the next section to construct an estimator. For this, we leverage semiparametric efficiency theory. Efficiency theory for low-dimensional functionals within semiparametric and nonparametric models was developed in a line of research including (Begun et al., 1983; Bickel et al., 1997; van der Vaart, 1998), among many others. (Kennedy, 2024) provides an excellent review oriented to causal inference.

The core step in the analysis is the derivation of a particular distributional Taylor expansion. For a functional $\theta : \mathcal{P} \rightarrow \mathbb{R}$, suppose that θ is sufficiently smooth so as to admit the following expansion, for any $\mathbb{P}_1, \mathbb{P}_2 \in \mathcal{P}$:

$$\theta(\mathbb{P}_1) = \theta(\mathbb{P}_2) - \mathbb{E}_{\mathbb{P}_2} \{ \varphi_\theta(Z; \mathbb{P}_1) \} + R(\mathbb{P}_1, \mathbb{P}_2), \quad (6)$$

where $\varphi_\theta : \mathcal{Z} \rightarrow \mathbb{R}$ is a mean-zero, finite-variance gradient and $R : \mathcal{P} \times \mathcal{P} \rightarrow \mathbb{R}$ is called the *second-order remainder*. In a nonparametric model, there is a unique gradient that characterizes the semiparametric efficiency bound, referred to as the *efficient influence function* (EIF) of θ . Importantly, R may only depend on \mathbb{P}_1 and \mathbb{P}_2 by their products or squares of their differences, justifying referring to R as second-order. We refer to (6) as the *von Mises expansion* of θ (von Mises, 1947), following the terminology used by Fernholz (1983); Robins et al. (2009); Kennedy (2024), among others.

The following theorem establishes that the smooth bounds in Proposition 2 admit von Mises expansions and characterizes their EIFs.

Theorem 1 (Efficient influence functions). *Under the setup of Proposition 2, suppose the maps $x \mapsto s_l(x, c, \gamma)$ and $x \mapsto s_g(x, c, \gamma)$ are twice-differentiable with bounded first and second derivatives. Let \dot{s} denote the first derivative. Then, the parameters $\psi_s(c, \gamma)$, $L_s(c, \gamma)$, and $U_s(c, \gamma)$ admit von-Mises expansions of the form (6), with, respectively, the following uncentered efficient influence functions:*

$$\begin{aligned} \varphi_\psi(Z, \eta, c, \gamma) &= \mu_1 s_g(\pi, c, \gamma) - \mu_0 s_l(\pi, 1 - c, \gamma) \\ &\quad + \frac{A}{\pi} s_g(\pi, c, \gamma) (Y - \mu_1) - \frac{1 - A}{1 - \pi} s_l(\pi, 1 - c, \gamma) (Y - \mu_0) \\ &\quad + \{ \mu_1 \dot{s}_g(\pi, c, \gamma) - \mu_0 \dot{s}_l(\pi, 1 - c, \gamma) \} (A - \pi), \\ \varphi_L(Z, \eta, c, \gamma) &= \varphi_{\psi_s}(Z, \eta, c, \gamma) - 1 + s_l(\pi, 1 - c, \gamma) + \dot{s}_l(\pi, 1 - c, \gamma) (A - \pi), \\ \varphi_U(Z, \eta, c, \gamma) &= \varphi_{\psi_s}(Z, \eta, c, \gamma) + 1 - s_g(\pi, c, \gamma) - \dot{s}_g(\pi, c, \gamma) (A - \pi). \end{aligned}$$

Theorem 1 provides the uncentered EIFs for the bounds. We will use them to construct debiased estimators in the next section. Beyond the assumptions of Proposition 2, we only require that the smooth approximation functions have bounded first and second derivatives with respect to their first argument, which can be guaranteed by construction, and is satisfied by the examples in Figure 1.

The efficient influence functions in Theorem 1 take the typical form of a plug-in plus weighted residuals. Starting with $\psi_s(c, \gamma)$, the first line of its EIF is the typical plug-in term that we could estimate and then average to obtain a plug-in estimator for $\psi_s(c, \gamma)$. The second and third lines include weighted residuals that debias the plug-in estimator. The third line is a debiasing term that arises due to the fact that the smoothed trimmed effect depends on the estimated propensity scores via the smoothing functions s_l and s_g . The second and third EIFs combine the EIF for $\psi_s(c, \gamma)$ with the EIFs for $1 - \mathbb{E} \{ s_g(\pi, c, \gamma) \}$ and $1 - \mathbb{E} \{ s_l(\pi, 1 - c, \gamma) \}$, respectively, and incorporate additional weighted residuals for debiasing estimators for $\mathbb{E} \{ s_l(\pi, 1 - c, \gamma) \}$ and $\mathbb{E} \{ s_g(\pi, c, \gamma) \}$.

Remark 2. The EIF φ_ψ of the smooth trimmed effect $\psi_s(c, \gamma)$ can be compared to the EIF of the ATE:

$$\mu_1 - \mu_0 + \left(\frac{A}{\pi} - \frac{1-A}{1-\pi} \right) (Y - \mu_A)$$

The key difference is that φ_ψ down-weights observations with extreme propensity scores through the smoothing functions s_l and s_g . This down-weighting occurs both in the plug-in terms and the inverse propensity weighted residuals.

4 Estimation of smooth bounds

In this section, we propose debiased estimators for the smooth bounds. With fixed threshold and smoothing parameters, we establish that our estimator is \sqrt{n} -consistent and asymptotically Gaussian under nonparametric conditions on the propensity score and outcome regression. Then, we demonstrate that the multiplier bootstrap facilitates asymptotically valid inference across a fixed finite set of parameters, and show how to use the multiplier bootstrap to obtain a narrower confidence interval.

A naive plug-in estimator would construct estimators for the nuisance functions in the identification result in Proposition 2 and plug them into the empirical average to approximate the expectation; e.g., a naive plug-in estimator for the lower bound $L_s(c, \gamma)$ would be

$$\hat{L}_s(c, \gamma) = \hat{\psi}_s(c, \gamma) - [1 - \mathbb{P}_n\{s_l(\hat{\pi}, 1 - c, \gamma)\}]$$

where

$$\hat{\psi}_s(c, \gamma) = \mathbb{P}_n\{\hat{\mu}_1 s_g(\hat{\pi}, c, \gamma) - \hat{\mu}_0 s_l(\hat{\pi}, 1 - c, \gamma)\}.$$

This plug-in estimator will inherit the convergence properties of the estimators for the outcome regression and propensity score. As a result, it can achieve \sqrt{n} -convergence with well-specified parametric models for the propensity score and outcome regression or with specific nonparametric assumptions. However, general guarantees are unavailable. In the previous section, we established that the smooth bounds are pathwise differentiable and admit EIFs. Therefore, here, we use the EIFs to debias the naive plug-in estimator, yielding new estimators that can converge at \sqrt{n} -rates under nonparametric assumptions.

4.1 Targeted learning

A variety of methods exist for constructing nonparametric asymptotically normal and efficient estimators of pathwise differentiable estimands, including estimating equations, one-step estimation, double machine learning, and targeted learning (Robins and Rotnitzky, 1995; Tsiatis, 2006; Chernozhukov et al., 2016; van der Laan and Robins, 2003; van der Laan and Rose, 2011). We focus on targeted learning because it is a substitution estimator which automatically yields estimates of the bounds that fall in $[-1, 1]$, unlike other approaches.

Targeted learning works by iteratively updating initial nuisance estimates $\hat{\eta}$ via a fluctuation model. The fluctuation model and loss function are carefully chosen to target the parameter of interest such that the final nuisance estimates $\hat{\eta}^*$ solve the empirical EIF estimating equation; e.g., when targeting the smooth lower bound $L_s(c, \gamma)$, the final estimates $\hat{\eta}^*$ satisfy

$$\mathbb{P}_n\{\varphi_L(Z_i, \hat{\eta}^*, c, \gamma)\} \approx 0.$$

This careful iteration debiases the resulting estimator, so that it has stronger convergence guarantees than the naive plug-in estimator. Nuisance estimation can be combined with sample splitting and cross-fitting to avoid Donsker or other complexity conditions in the analysis (Chernozhukov et al., 2018; Zheng and van der Laan, 2011; Chen et al., 2022). For simplicity of presentation in this section, we assume only sample splitting is used, where nuisance estimates are constructed on a separate fold of n samples. However, in practice we employ cross-fitting and cycle through the folds to retain full sample efficiency.

4.1.1 Fluctuation model and loss function

For the specific Targeted Minimum Loss-based Estimator (TMLE) we propose, we use the following fluctuation model and loss function, which can be seen as an extension of those in Gruber and van der Laan (2010). For $\epsilon \in \mathbb{R}$,

$$\begin{aligned}\hat{\mu}_0(\epsilon) &= \text{logit}^{-1} \left\{ \text{logit}(\mu_0) + \frac{1}{1-\pi} s_l(\pi, 1-c, \gamma) \times \epsilon \right\}, \\ \hat{\mu}_1(\epsilon) &= \text{logit}^{-1} \left\{ \text{logit}(\mu_1) + \frac{1}{\pi} s_g(\pi, c, \gamma) \times \epsilon \right\}, \text{ and} \\ \hat{\pi}(\epsilon) &= \text{logit}^{-1} \left[\text{logit}(\pi) + \{\mu_1 \dot{s}_g(\pi, c, \gamma) - \mu_0 \dot{s}_l(\pi, 1-c, \gamma) + M\} \times \epsilon \right],\end{aligned}$$

where $M = \dot{s}_l(\pi, 1-c, \gamma)$ when targeting a lower bound $L_s(c, \gamma)$ and $M = -\dot{s}(\pi > c)$ when targeting an upper bound $U_s(c, \gamma)$. These fluctuation models satisfy the key property that at $\epsilon = 0$, each fluctuation reduces to μ_0 , μ_1 , and π , respectively. We then use the following loss function:

$$\begin{aligned}\mathcal{L}(\epsilon, Z) &= -A \log \hat{\pi}(\epsilon) - (1-A) \log \{1 - \hat{\pi}(\epsilon)\} \\ &\quad - A \left[Y \log \hat{\mu}_1(\epsilon) + (1-Y) \log \{1 - \hat{\mu}_1(\epsilon)\} \right] \\ &\quad - (1-A) \left[Y \log \hat{\mu}_0(\epsilon) + (1-Y) \log \{1 - \hat{\mu}_0(\epsilon)\} \right].\end{aligned}$$

This loss function satisfies the key property that the EIF of the target parameter is contained in the linear span of the gradient of the loss function with respect to ϵ evaluated at $\epsilon = 0$. This ensures that the fluctuation step reduces bias toward the target parameter in the optimal direction, guaranteeing asymptotically efficient estimation. This fluctuation model and loss function can be used for both a bounded continuous outcome ($Y \in [0, 1]$) and a binary outcome $Y \in \{0, 1\}$.

4.1.2 Targeted Minimum Loss-based Estimator

With the fluctuation model and loss function in hand, we next outline the TMLE. We focus on estimating $L_s(c, \gamma)$. An almost identical algorithm is used to estimate $U_s(c, \gamma)$, but where M is changed in the fluctuation submodel.

Algorithm 1 (TMLE). *Assume access to initial nuisance estimates $\hat{\eta}$ learned on a separate, independent, sample.*

1. *Initialization:* set $\hat{\eta}^* = \hat{\eta}$.
2. *Loss minimization:* find ϵ^* by empirical minimization of \mathcal{L} under the fluctuation model conditional on nuisance parameter estimates $\hat{\eta}^*$:

$$\epsilon^* = \underset{\epsilon \in \mathbb{R}}{\text{argmin}} \sum_{i=1}^n \mathcal{L}(\epsilon, Z_i)$$

3. *Recursive update: set nuisance parameter estimates $\widehat{\eta}^* = \widehat{\eta}(\epsilon^*)$.*
4. *Repeat Steps 2-3 until convergence (i.e. when $\epsilon^* \approx 0$).*
5. *Using the final nuisance estimates from step 3, construct debiased plug-in estimators*

$$\widehat{L}_s(c, \gamma) = \widehat{\psi}_s(c, \gamma) - [1 - \mathbb{P}_n\{s_l(\widehat{\pi}^*, 1 - c, \gamma)\}]$$

and

$$\widehat{U}_s(c, \gamma) = \widehat{\psi}_s(c, \gamma) + [1 - \mathbb{P}_n\{s_g(\widehat{\pi}^*, c, \gamma)\}]$$

where

$$\widehat{\psi}_s(c, \gamma) = \mathbb{P}_n\{\widehat{\mu}_1^* s_g(\widehat{\pi}^*, c, \gamma) - \widehat{\mu}_0^* s_l(\widehat{\pi}^*, 1 - c, \gamma)\}.$$

Meanwhile, construct variance estimates $\widehat{\sigma}_L^2$ and $\widehat{\sigma}_U^2$ using the unbiased sample variance of $\varphi_L(Z, \widehat{\eta}^*, c, \gamma)$ and $\varphi_U(Z, \widehat{\eta}^*, c, \gamma)$, respectively.

4.1.3 Convergence guarantees

The following result establishes convergence of the TMLE to a Gaussian limiting distribution centered on the truth.

Theorem 2 (Weak convergence, fixed c, γ). *Fix $c \in [0, \frac{1}{2}]$, $\gamma \in (0, \infty)$. Assume the nuisance convergence rates $\|\widehat{\pi} - \pi\| = o_{\mathbb{P}}(n^{-1/4})$, $\|\widehat{\mu}_0 - \mu_0\| = o_{\mathbb{P}}(n^{-1/4})$, and $\|\widehat{\mu}_1 - \mu_1\| = o_{\mathbb{P}}(n^{-1/4})$. Then*

$$\frac{\sqrt{n}}{\widehat{\sigma}_L} \left(\widehat{L}_s(c, \gamma) - L_s(c, \gamma) \right) \rightsquigarrow N(0, 1) \quad \text{and} \quad \frac{\sqrt{n}}{\widehat{\sigma}_U} \left(\widehat{U}_s(c, \gamma) - U_s(c, \gamma) \right) \rightsquigarrow N(0, 1).$$

Theorem 2 provides the key convergence guarantee for our TMLE in Algorithm 1. Notably, unlike with the TMLE for the ATE, this result does not require the strong overlap assumption that π or $\widehat{\pi}$ are bounded away from zero and one (with the tradeoff that without the overlap assumption, the TMLE can only estimate bounds for the ATE, and not a point estimate). The theorem demonstrates that if the nuisance functions—the propensity score and outcome regressions—are estimated at $n^{-1/4}$ rates in root mean squared error, then our estimators for the smooth lower and upper bounds converge at \sqrt{n} -rates to the true bounds with Gaussian limiting distributions. Moreover, these estimators achieve the nonparametric efficiency bound, which is the variance of each bound's EIF. These nuisance convergence rate assumptions can be satisfied using flexible nonparametric estimators under standard regularity conditions such as smoothness or sparsity (Györfi et al., 2002).

4.1.4 Confidence interval for the ATE

Theorem 2 suggests a straightforward confidence interval for the ATE, as the intersection of $1 - \alpha/2$ one-sided intervals for the lower and upper bounds:

$$\left[\widehat{L}_s(c, \gamma) - q_{1-\alpha/2} \sqrt{\frac{\widehat{\sigma}_L^2}{n}}, \widehat{U}_s(c, \gamma) + q_{1-\alpha/2} \sqrt{\frac{\widehat{\sigma}_U^2}{n}} \right].$$

This confidence interval obtains valid coverage for the ATE by Theorem 2, Proposition 2, and a union bound.

In fact, it may be possible to reduce the critical values used to construct the confidence interval, following the procedure in Imbens and Manski (2004). The intuition is that the ATE cannot be close to both the lower and upper bounds when they are well separated, and therefore one can consider the intersection of $1 - \alpha$ one-sided intervals. Saving this approach for future work, we instead extend our approach to hold simultaneously over a finite set of parameters, next.

4.2 Valid inference and narrow confidence intervals with many parameters

In the previous section, we established asymptotic guarantees for a fixed threshold parameter c and smoothing parameter γ . However, in practice, researchers face tradeoffs when choosing a parameter combination: smaller c and γ will give tighter bounds, but these can be more difficult to estimate, leading to a wider CI. Therefore, rather than forcing researchers to commit to a single parameter combination, we develop inferential methods that hold uniformly over a finite set of parameters. This approach allows researchers to prespecify a set of plausible parameter combinations and then use *the narrowest confidence interval* that maintains valid coverage across all choices.

In the following algorithm, we assume as input a set of finite parameters: $\mathcal{C} = \{(c_1, \gamma_1), \dots, (c_K, \gamma_K)\}$, where $|\mathcal{C}| = K$. For brevity, we'll omit (c_k, γ_k) arguments, and instead use k subscripts. For example, we will let $\widehat{L}_k \equiv \widehat{L}_s(c_k, \gamma_k)$ and $\widehat{\sigma}_{L,k} \equiv \widehat{\sigma}_L(c_k, \gamma_k)$. We use a multiplier bootstrap to simulate the joint distribution of all bound estimators, then calibrate our confidence intervals using the most extreme realization across all parameter combinations. This ensures that even after selecting the narrowest interval, we have appropriate coverage.

Algorithm 2. *Given K threshold and smooth parameter combinations $\{(c_k, \gamma_k)\}_{k=1}^K$:*

1. *For each $k \in [K]$, construct efficient influence function estimates as in the prior section: $\{\varphi_{L,k}(Z_i, \widehat{\eta}), \varphi_{U,k}(Z_i, \widehat{\eta})\}_{i=1}^n$. Also construct point estimates and standard error estimators for the upper and lower bounds: $\{\widehat{L}_k, \widehat{U}_k\}$ and $\{\widehat{\sigma}_{L,k}, \widehat{\sigma}_{U,k}\}$.*
2. *For B bootstrap samples, draw i.i.d. multipliers $\{\xi_i^{(b)}\}_{i=1}^n$ with $\mathbb{E}(\xi) = 0$, $\mathbb{E}(\xi^2) = 1$, and form the studentized residuals for each index k :*

$$T_{L,k}^{(b)} = \frac{1}{\sqrt{n}} \sum_{i=1}^n \xi_i^{(b)} \left\{ \frac{\varphi_{L,k}(Z_i, \widehat{\eta}) - \widehat{L}_k}{\widehat{\sigma}_{L,k}} \right\}, \quad T_{U,k}^{(b)} = \frac{1}{\sqrt{n}} \sum_{i=1}^n \xi_i^{(b)} \left\{ \frac{\varphi_{U,k}(Z_i, \widehat{\eta}) - \widehat{U}_k}{\widehat{\sigma}_{U,k}} \right\}.$$

3. *Compute the bootstrap max-max statistic*

$$\widehat{M}^{(b)} := \max_{1 \leq k \leq K} \max \left(T_{L,k}^{(b)}, -T_{U,k}^{(b)} \right).$$

Let $\widehat{q}_{1-\alpha}$ be the empirical $(1 - \alpha)$ quantile of $\{\widehat{M}^{(b)}\}_{b=1}^B$.

4. *Construct a uniform confidence set across all parameter sets as*

$$\left\{ \left[\widehat{L}_k - \widehat{q}_{1-\alpha} \widehat{\sigma}_{L,k}, \widehat{U}_k + \widehat{q}_{1-\alpha} \widehat{\sigma}_{U,k} \right] \right\}_{k=1}^K.$$

5. *Construct the narrowest confidence interval for the ATE as*

$$\widehat{CI} = \left[\max_k \widehat{L}_k - \widehat{q}_{1-\alpha} \widehat{\sigma}_{L,k}, \min_k \widehat{U}_k + \widehat{q}_{1-\alpha} \widehat{\sigma}_{U,k} \right].$$

Algorithm 2 combines the TMLE in Algorithm 1 with the multiplier bootstrap. It outputs two quantities: a uniform confidence set across all parameters, and the narrowest CI for the ATE. A key feature of our approach is the construction of the max-max statistic using only one side of each studentized residual: $T_{L,k}$ for lower bounds and $-T_{U,k}$ for upper bounds. This asymmetric construction reflects the different types of estimation errors we seek to control. For the lower bounds, the relevant error event is over-estimation (when \widehat{L}_k exceeds the true L_k), which corresponds to positive deviations in $T_{L,k}$. For the upper bounds, the critical error is under-estimation (when \widehat{U}_k falls below the true U_k), corresponding to negative deviations in $T_{U,k}$. By incorporating only the relevant tail of each distribution, this construction yields one-sided simultaneous confidence bands that cover the set $[L_{\max}, U_{\min}]$ with the desired coverage probability.

The next result establishes that the uniform set and narrowest CI facilitate asymptotically valid inference.

Theorem 3. *Suppose the conditions of Theorem 2 hold and a uniform confidence set and narrow confidence interval are constructed according to Algorithm 2. Further suppose $\widehat{\sigma}_{L,k} \xrightarrow{p} \sigma_{L,k}$ and $\widehat{\sigma}_{U,k} \xrightarrow{p} \sigma_{U,k}$ for all $k \in [K]$. Then,*

$$\mathbb{P} \left\{ \forall k \in [K], \mathbb{E}(Y^1 - Y^0) \in \left[\widehat{L}_k - \widehat{q}_{1-\alpha} \widehat{\sigma}_{L,k}, \widehat{U}_k + \widehat{q}_{1-\alpha} \widehat{\sigma}_{U,k} \right] \right\} \geq 1 - \alpha + o_{\mathbb{P}}(1).$$

Moreover,

$$\mathbb{P} \left\{ \mathbb{E}(Y^1 - Y^0) \in \widehat{CI} \right\} \geq 1 - \alpha + o_{\mathbb{P}}(1).$$

Theorem 3 establishes the key inferential guarantees. First, it shows that the uniform confidence set attains valid coverage across all bounds. As a result, the narrowest CI for the ATE, constructed using the maximum lower CI bound and minimum upper CI bound, also maintains valid coverage. The crucial caveat is that this comes at a cost: the critical value $\widehat{q}_{1-\alpha}$ will be larger than its pointwise counterpart. In practice, we have seen roughly 10% increases (e.g., from 1.96 to approximately 2.1) with $K = 162$. This tradeoff is valuable when researchers are uncertain about the optimal balance between smooth approximation error and estimator variance, and this balance varies substantially across the parameter space. Conversely, when prior analyses or diagnostic tools provide clear guidance toward a single parameter combination, the pointwise estimators from the prior section are preferable.

5 Simulation Study

The simulation study compares the non-overlap bounds to a doubly-robust estimator of the ATE in a setting designed to exhibit extreme non-overlap. As a benchmark, we applied a doubly-robust one-step estimator based on the uncentered EIF of ATE, which is

$$\phi(Z) = \mu_1 - \mu_0 + \left(\frac{A}{\pi} - \frac{1-A}{1-\pi} \right) (Y - \mu_A).$$

The one-step estimator is

$$\hat{\psi}^{\text{dr}} = \frac{1}{n} \sum_{i=1}^n \hat{\phi}(Z_i), \tag{7}$$

where $\hat{\phi}$ is an estimate of the uncentered EIF. Asymptotically valid 95% confidence intervals are formed as $\hat{\psi}^{\text{dr}} \pm q_{0.975} \sqrt{\text{var}(\hat{\phi}_\psi)/n}$, where $q_{0.975}$ is the 97.5% quantile of the standard normal distribution and $\text{var}(\hat{\phi}_\psi)$ is the empirical variance of the estimated uncentered EIF. The width of the one-step 95% confidence interval is $W^{\text{dr}} = \min(2, (q_{0.975} - q_{0.025}) \sqrt{\text{var}(\hat{\phi}_\psi)/n})$. We truncated the width to have a maximum of 2, indicating the interval covered the entire parameter space. We rejected the null hypothesis of that the ATE equals zero if the estimated 95% confidence interval excluded zero.

The non-overlap ATE bounds were estimated with a logarithmic grid of propensity score thresholds from $c = 10^{-4}$ to $c = 0.05$. The non-overlap bounds were estimated for each of the smoothness parameters $\gamma \in \{10^{-3}, 10^{-2}, 10^{-1}\}$. A uniform 95% confidence set over the thresholds and smoothness parameters was calculated using the proposed multiplier bootstrap method with 1000 bootstrap draws. For comparison with the one-step estimator, the uncertainty interval width for the non-overlap ATE bounds at each γ was taken to be the tightest uniform 95% confidence interval over the tested propensity score thresholds, also truncated to have maximum of 2: $W_\gamma^{\text{robust}} = \min(2, \min_c \hat{U}_s(c, \gamma) - \min_c \hat{L}_s(c, \gamma))$. We rejected the null hypothesis of a null treatment effect if any of the uniform 95% confidence intervals over the propensity score thresholds excluded zero.

We compared the finite-sample performance of the one-step estimator and non-overlap bounds with respect to a data-generating process (DGP) designed to exhibit extreme practical overlap violations. Simulated datasets are composed of n i.i.d. copies of $Z = (X_1, X_2, A, Y)$ drawn from the joint law characterized by

$$\begin{aligned} X_1 &\sim \text{Uniform}(-1, 1), \\ X_2 &\sim \text{Categorical}(\{-1, 0, 1\}, \{0.05, 0.9, 0.05\}), \\ A | X &\sim \text{Bernoulli}(\text{logit}^{-1}(X_1 + \alpha \times X_2)), \\ Y | A, X &\sim \text{Bernoulli}(\text{logit}^{-1}(0.5 + X_1 + A)), \end{aligned} \tag{8}$$

where α controls the severity of non-overlap. For the main simulation study we set $\alpha = 5$ to induce extreme positivity violations. In Appendix B, we present results for simulations with $\alpha = 1$ to evaluate the non-overlap bounds in a setting where overlap is satisfied. The true ATE under the DGP above is $\psi \approx 0.227$.

The sampling distribution of doubly-robust estimators of the ATE can be highly skewed under DGPs exhibiting extremely variable propensity scores (Robins et al., 2007). For the one-step estimator (7), the reason this occurs can be easily seen by analyzing the term involving inverse propensity weights of the uncentered EIF. Define the observed inverse propensity weight as

$$r_i = \left(\frac{A_i}{\pi(X_i)} - \frac{1 - A_i}{1 - \pi(X_i)} \right), \tag{9}$$

which enters into the one-step estimator by weighting the residual, $Y - \mu_A(X)$ (see eq. (7)). The residual will be non-zero assuming that the conditional variance of Y given A and X is non-zero. For the inverse propensity weight r_i to be large, there must be an observation with both $A_i = 1$ and $\pi(X_i)$ small, or $A_i = 0$ and $1 - \pi(X_i)$ small. By definition, it is unlikely to observe $A = 1$ when $\pi(X)$ is small (likewise for the opposite case). In the rare event that this occurs, then r_i is large, causing high variance in the estimator and skewness of the sampling distribution. In addition, the empirical variance of the estimated EIF will be large, leading to uninformative confidence intervals.

The skewness of the sampling distributions of doubly-robust estimators due to overlap violations complicates characterizing their behavior in simulation studies. Robins et al. (2007) made this point in their response to Kang and Schafer (2007), arguing that “one thousand replications are not enough to capture the tail behavior of highly skewed sampling distributions, and as such cannot produce reliable Monte Carlo estimates of bias, much less of variance.” One approach to reduce the Monte Carlo error would be to simply increase the number of replications; we do so by running 1000 replications.

In addition to increasing the number of simulation replications, we address the issue of highly skewed sampling distributions in two ways. First, we conditionally simulate datasets that exhibit non-overlap. Specifically, we draw datasets from (8) via rejection sampling such that $\max_i |r_i| > 100$. That is, datasets of size n are drawn repeatedly until a dataset is found that has at least one observation with $A_i = 1$ and $\pi(X_i) < 0.01$ or $A_i = 0$ and $\pi(X_i) > 0.99$ (which each imply $|r_i| > 100$). This targets the investigation to the datasets with extreme non-overlap that cause particular problems for traditional estimators. This helps us to characterize the “worst-case” performance of traditional estimators. For context, we also perform a simulation study that is identical except for using unconditional draws from (8), without rejection sampling. This allows us to characterize the “average” performance of the estimators with respect to our DGP.

The second way we address skewed sampling distributions under non-overlap is by evaluating our methods with additional metrics that capture the full sampling distribution. For the 95% uncertainty interval widths of the one-step and non-overlap bounds, we calculate their means, 90% quantiles, and standard deviation across simulations to capture both the central tendency and spread of the sampling distributions. We also report traditional metrics including the empirical coverage of the 95% confidence intervals and the power of the hypothesis tests, defined as the proportion of simulations in which each method rejected the null hypothesis of a null treatment effect.

We generated 5000 simulation datasets for every sample size $n \in \{100, 250, 500, 1000\}$ via the rejection sampling (such that simulation datasets have $\max_i |r_i| > 100$) and non-rejection sampling methods described above. In all cases, nuisance parameters for both the benchmark one-step estimator and the non-overlap bounds were estimated using well-specified generalized linear models and 5-fold sample splitting.

We emphasize that we did not compare the non-overlap bounds to methods targeting alternative estimands, such as overlap weighting (Li et al., 2018a) or propensity score trimming (Crump et al., 2009; McClean and Díaz, 2025) precisely because our inferential goal is to estimate the *population* ATE, and not an alternative estimand. Because propensity score trimming, for example, does not target the ATE, it is not a relevant comparator to non-overlap bounds. For comparisons of the finite-sample performance of various weighting and trimming estimators, we refer to the substantial literature on the subject (Stürmer et al., 2010; Lee et al., 2011; Busso et al., 2014; Li et al., 2018b; Zhou et al., 2020; Stürmer et al., 2021; Ben-Michael and Keele, 2023).

Results The results of the simulation study are shown in Table 1, focusing on uncertainty interval widths, and Table 2, containing empirical coverage and power results. Each table is separated into separate sections for (A) the simulations generated conditional on $\max_i |r_i| > 100$ and (B) simulations generated unconditionally. The estimators exhibit significantly difference performance in the conditionally simulated simulations, which we emphasize represents the “worst-case” behavior of traditional doubly-robust estimators by targeting the skewed region of their sampling distributions. As expected, in this regime the 95% confidence interval widths for the doubly-robust one-step estimator are wide on average, and are highly variable. Coverage is conservative, reaching near

100% coverage. Power to reject the null hypothesis is low; at the smallest sample size $n = 100$, the null hypothesis is rejected in only 3% of simulations. In comparison, the non-overlap bounds are narrower and are less variable at all sample sizes and choice of tuning parameter γ . The non-overlap bounds also exhibit higher power; for example achieving approximately 50% power at the smallest sample size of $n = 100$.

In the unconditional regime, representing the “average-case” performance of the estimators under the simulation DGP, the non-overlap bounds have smaller mean width and are less variable than the doubly-robust uncertainty intervals. On the other hand, the doubly-robust intervals exhibit better empirical coverage and power in this scenario. The non-overlap bounds nevertheless achieve higher power for some sample sizes. That the doubly-robust one-step estimator performs better in this regime compared to the previous conditional regime can be explained by the skewness of its sampling distribution. By marginalizing over the entire sampling distribution, poor behavior when extreme finite-sample overlap violations occur (i.e. $\max_i |r_i|$ is large) is de-emphasized. The skewness also explains the relationships that the mean and median confidence intervals widths have with increasing sample size: the mean width *increases* with sample size, while the median *decreases*, because larger simulated datasets have higher probability of including an observation with a large r_i value.

The non-overlap bounds in the both simulation regimes were slightly sensitive to the choice of tuning parameter γ . As expected by the construction of the bounds, the mean interval width slightly increased and empirical coverage became more conservative as the smoothness parameter increased.

6 Application

To illustrate the utility of our methods we reanalyze data from an observational study of mortality following treatment with right heart catheterization (RHC) among patients in five medical centers in the USA (Murphy and Cluff, 1990; Connors et al., 1996). Formally, the treatment is defined as whether RHC was applied within 24 hours of hospital admission (with $A = 1$ indicating treatment and $A = 0$ non-treatment). The outcome is a binary indicator of survival at 30 days post admission. The covariates comprise 72 variables. The dataset includes $n = 5735$ patients, with 2184 in the treatment group and 3551 in the non-treatment group. Due to significant differences in the covariate distribution between groups, these data have been reanalyzed numerous times to illustrate causal inference methods designed to address practical overlap violations (Hirano and Imbens, 2001; Crump et al., 2009; Traskin and Small, 2011; Rosenbaum, 2012; Li et al., 2018a; Rothe, 2017; Lee and Weidner, 2021b; Ma et al., 2024). For our analysis, we use the version of the dataset publicly available in the R package **ATbounds** (Lee and Weidner, 2021a).

We calculated the non-overlap bounds on a logarithmic grid from $c = 10^{-6}$ to $c = 10^{-1}$. The smoothness tuning parameter was set to each of the values $\gamma \in \{0.001, 0.01\}$. A uniform 95% confidence set over the grid of thresholds and both tuning parameter values was calculated using the multiplier bootstrap method with 1000 bootstrap draws. Nuisance parameters were estimated using cross-fitted generalized linear models with 5 folds. Replication material in the form of an R script is available in Appendix C.

The estimated uniform non-overlap 95% bounds for $\gamma = 0.01$ are shown in Figure 2 (a comparable plot for $\gamma = 0.001$ is included in the appendix). The uniform non-overlap bounds exclude zero for a subset of the propensity score thresholds, implying statistically significant evidence of a non-zero ATE at the 5% level. The tightest uniform 95% uncertainty interval for the ATE was $(-0.03, -0.10)$.

N	γ	95% UI Width									
		Mean		Median		90% Quantile		Std. Dev.		Bounds	DR
		Bounds	DR	Bounds	DR	Bounds	DR	Bounds	DR		
<i>(A) Simulations conditional on $\max_i r_i > 100$</i>											
100	10^{-3}	0.46	1.91	0.45	2.00	0.51	2.00	0.05	0.36		
	10^{-2}	0.46	1.91	0.45	2.00	0.51	2.00	0.06	0.36		
	10^{-1}	0.49	1.91	0.49	2.00	0.57	2.00	0.06	0.36		
250	10^{-3}	0.29	1.83	0.28	2.00	0.32	2.00	0.03	0.49		
	10^{-2}	0.29	1.83	0.29	2.00	0.32	2.00	0.04	0.49		
	10^{-1}	0.37	1.83	0.37	2.00	0.40	2.00	0.03	0.49		
500	10^{-3}	0.22	1.65	0.21	2.00	0.28	2.00	0.05	0.68		
	10^{-2}	0.23	1.65	0.22	2.00	0.27	2.00	0.04	0.68		
	10^{-1}	0.29	1.65	0.29	2.00	0.31	2.00	0.02	0.68		
1000	10^{-3}	0.17	1.35	0.15	2.00	0.23	2.00	0.07	0.84		
	10^{-2}	0.20	1.35	0.20	2.00	0.24	2.00	0.04	0.84		
	10^{-1}	0.23	1.35	0.23	2.00	0.25	2.00	0.01	0.84		
<i>(B) Unconditional simulations</i>											
100	10^{-3}	0.51	0.52	0.50	0.41	0.58	0.51	0.06	0.39		
	10^{-2}	0.51	0.52	0.50	0.41	0.58	0.51	0.06	0.39		
	10^{-1}	0.51	0.52	0.51	0.41	0.58	0.51	0.05	0.39		
250	10^{-3}	0.34	0.54	0.34	0.25	0.37	2.00	0.04	0.66		
	10^{-2}	0.34	0.54	0.34	0.25	0.37	2.00	0.03	0.66		
	10^{-1}	0.35	0.54	0.35	0.25	0.38	2.00	0.02	0.66		
500	10^{-3}	0.25	0.67	0.26	0.17	0.29	2.00	0.03	0.81		
	10^{-2}	0.26	0.67	0.26	0.17	0.29	2.00	0.03	0.81		
	10^{-1}	0.28	0.67	0.28	0.17	0.30	2.00	0.02	0.81		
1000	10^{-3}	0.19	0.90	0.20	0.19	0.23	2.00	0.04	0.91		
	10^{-2}	0.21	0.90	0.21	0.19	0.23	2.00	0.03	0.91		
	10^{-1}	0.23	0.90	0.23	0.19	0.24	2.00	0.01	0.91		

Table 1: Uncertainty width results from Simulation Study 1 (Section 5) for (A) simulations conditional on $\max_i |r_i| > 100$, with r_i the inverse propensity weight defined in (9), and (B) simulations generated unconditionally. Results compare the 95% uncertainty intervals of a doubly-robust one-step estimator (DR) and the tightest uniform 95% non-overlap bounds (Bounds) across a grid of propensity score thresholds and smoothness parameters in terms of the mean, median, 90%, quantile, and standard deviation of the uncertainty interval width.

N	γ	95% Coverage		Power	
		Bounds	DR	Bounds	DR
<i>(A) Simulations conditional on $\max_i r_i > 100$</i>					
100	10^{-3}	96.4%	99.9%	0.49	0.02
	10^{-2}	96.5%	99.9%	0.49	0.02
	10^{-1}	98.1%	99.9%	0.43	0.02
250	10^{-3}	96.9%	99.5%	0.88	0.07
	10^{-2}	97.0%	99.5%	0.88	0.07
	10^{-1}	99.5%	99.5%	0.71	0.07
500	10^{-3}	97.5%	99.1%	1.00	0.16
	10^{-2}	98.3%	99.1%	0.99	0.16
	10^{-1}	99.9%	99.1%	0.95	0.16
1000	10^{-3}	97.8%	98.8%	1.00	0.31
	10^{-2}	99.3%	98.8%	1.00	0.31
	10^{-1}	99.9%	98.8%	1.00	0.31
<i>(B) Unconditional simulations</i>					
100	10^{-3}	98.5%	93.8%	0.35	0.52
	10^{-2}	98.4%	93.8%	0.35	0.52
	10^{-1}	98.7%	93.8%	0.35	0.52
250	10^{-3}	98.9%	93.8%	0.78	0.78
	10^{-2}	99.0%	93.8%	0.78	0.78
	10^{-1}	99.4%	93.8%	0.74	0.78
500	10^{-3}	99.0%	95.0%	0.98	0.72
	10^{-2}	99.4%	95.0%	0.98	0.72
	10^{-1}	99.8%	95.0%	0.96	0.72
1000	10^{-3}	98.6%	95.8%	1.00	0.57
	10^{-2}	99.7%	95.8%	1.00	0.57
	10^{-1}	99.9%	95.8%	1.00	0.57

Table 2: Empirical coverage and power results from Simulation Study 1 (Section 5) for (A) simulations conditional on $\max_i |r_i| > 100$, with r_i the inverse propensity weight defined in (9), and (B) simulations generated unconditionally. Results compare the 95% uncertainty intervals of a doubly-robust one-step estimator (DR) and the tightest uniform 95% non-overlap bounds (Bounds) across a grid of propensity score thresholds and smoothness parameters in terms of empirical 95% coverage and power.

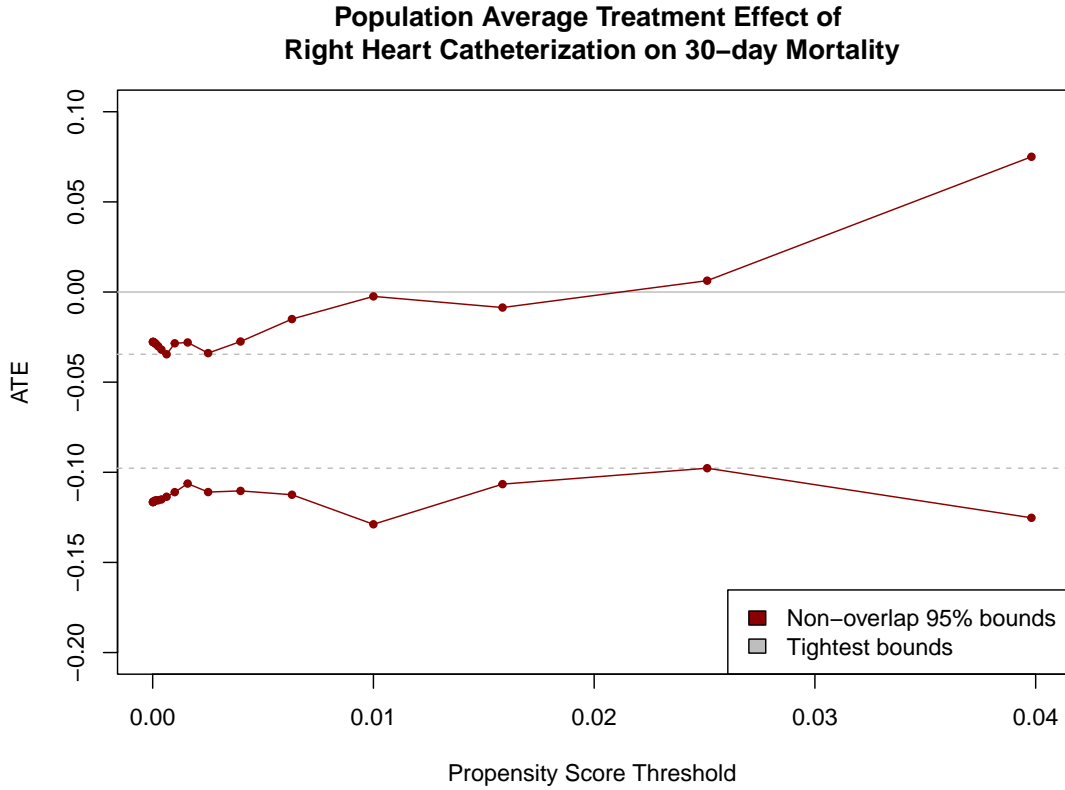


Figure 2: Uniform 95% non-overlap bounds (for $\gamma = 0.01$) on the average treatment effect (ATE) of right heart catheterization on survival. The points illustrate the lower and upper bounds with respect to a logarithmic grid of propensity score thresholds. The lines between points are solely to guide the eye. The horizontal dotted lines indicate the tightest valid 95% uncertainty interval that may be formed from the non-overlap bounds.

In comparison, a doubly-robust one-step point estimate of the ATE has 95% confidence intervals that are non-informative (covering the entire parameter space $[-1, 1]$) due to the presence of observations with large inverse propensity weights.

The estimated non-overlap bounds for the ATE are consistent with previous point estimates of alternative treatment effects defined via weighting or exclusion to target subpopulations satisfying overlap. To illustrate, the estimates reported in (Crump et al., 2009) for the treatment effect among the population with propensity score estimates in $[0.1, 0.9]$ fall within the non-overlap bounds, as do the estimated overlap treatment effect reported in Li et al. (2018b). As opposed to their results, however, our results allow for inference on the ATE.

7 Discussion

In practice, our results have implications for Average Treatment Effect (ATE) estimation when there are structural or practical violations of the overlap assumption. Under structural overlap violations, our method facilitates valid statistical inference for the ATE even when it is not point identified. Under practical violations, our method can facilitate more precise inference. This is in contrast

to alternative approaches, which achieve point identification or precise estimation by changing the target of interest and thus altering the scientific question of interest (Petersen and van der Laan, 2014; Dang et al., 2023; Rizk, 2025). Therefore, if the estimand of interest is the ATE and not a weighted or trimmed alternative, then our methods provide a novel solution to conduct inference on the target of interest. From this view, alternative weighted or trimmed estimands can be part of a *secondary* subgroup analysis, and reported in addition to non-overlap bounds, which provide important context about what is known about the ATE.

The performance of the non-overlap bounds in finite samples with practical non-overlap is surprising in that the bounds may have better properties than classical confidence intervals derived for an asymptotically efficient and doubly-robust point estimator of the ATE. Lest we be charged with offering a free lunch, we emphasize that the use of non-overlap bounds involves tradeoffs. First, in exchange for overlap we require outcome boundedness. Second, non-overlap bounds sacrifice point identification in exchange for partial identification bounds. Finally, non-overlap bounds are informative only in specific scenarios. The width of the non-overlap bounds is a function of the size of the non-overlap subpopulation, and the bounds will exclude zero only if the size of that population (representing “noise”) is smaller than the treatment effect in the overlap subpopulation (representing “signal”). The core insight of our work is that, in our experience as applied researchers, in many real-world situations the non-overlap population is small, meaning that the non-overlap bounds may still yield sufficiently narrow bounds to be useful.

Practical use of the non-overlap bounds requires setting an additional tuning parameter beyond those required for traditional doubly-robust estimators, in the form of the smooth approximation parameter γ . In the simulation study, the performance of non-overlap bounds was not highly sensitive to γ , suggesting that in practice a small value can be chosen, such as $\gamma = 10^{-2}$ or 10^{-3} . Following Branson et al. (2024), who apply a similar type of smooth approximation in a different context, we advise testing multiple values of γ in a sensitivity analysis. The strength of the uniform non-overlap bounds formed via the multiplier bootstrap is that they are valid over all specified combinations of threshold and smoothness parameter, allowing for valid inference even when multiple smoothness parameters are used. In addition, an interesting avenue for future work is to consider uniform inference methods valid for both non-overlap bounds and confidence intervals for point estimates of the ATE. Indeed, when the threshold $c = 0$ and the smoothness is set to $\lambda = 0$, then the non-overlap bounds are equivalent (in practice) to a classical Wald-type confidence interval around a TMLE point estimate of the ATE. A combined inference approach would allow for fully pre-specified analysis plans that are both robust to overlap violations while yielding point estimates when overlap is satisfied.

While we focused on deriving non-overlap bounds for the ATE, as a canonical example, we expect that our approach is relevant to a larger class of causal estimands. The two key ingredients necessary are a bounded outcome and overlap violations within a small proportion of the population relative to the magnitude of the treatment effect in the rest of the population. We suspect that continuous treatment effects (Schomaker et al., 2024), longitudinal treatment effects (McClean and Díaz, 2025), and transport treatment effects (Zivich et al. 2024a,b) may be particularly amenable to this style of data-adaptive non-overlap bounds.

Declaration of the use of generative AI and AI-assisted technologies

During the preparation of this work the authors used ChatGPT in order to suggest edits for grammar and clarity. After using this tool/service the authors reviewed and edited the content as necessary and take full responsibility for the content of the publication.

Acknowledgements

The computational requirements for this work were supported in part by the NYU Langone High Performance Computing (HPC) Core's resources and personnel.

Data Availability

Replication materials for the simulation study and data application are available at https://github.com/herbps10/robust_ate_bounds_paper. An R package implementing the proposed estimators is available at <https://github.com/herbps10/effectbounds>.

References

Begin, J. M., Hall, W., Huang, W.-M., Wellner, J. A., et al. (1983). Information and asymptotic efficiency in parametric-nonparametric models. *The Annals of Statistics*, 11(2):432–452.

Ben-Michael, E. and Keele, L. (2023). Using balancing weights to target the treatment effect on the treated when overlap is poor. *Epidemiology*, 34(5).

Bickel, P. J., Klaassen, C. A., Ritov, Y., and Wellner, J. A. (1997). *Efficient and Adaptive Estimation for Semiparametric Models*. Springer-Verlag.

Bonvini, M. and Kennedy, E. H. (2022). Sensitivity analysis via the proportion of unmeasured confounding. *Journal of the American Statistical Association*, 117(539):1540–1550.

Branson, Z., Kennedy, E. H., Balakrishnan, S., and Wasserman, L. (2024). Causal effect estimation after propensity score trimming with continuous treatments.

Busso, M., DiNardo, J., and McCrary, J. (2014). New evidence on the finite sample properties of propensity score reweighting and matching estimators. *The Review of Economics and Statistics*, 96(5):885–897.

Chen, Q., Syrgkanis, V., and Austern, M. (2022). Debiased machine learning without sample-splitting for stable estimators. *Advances in Neural Information Processing Systems*, 35:3096–3109.

Chernozhukov, V., Chetverikov, D., Demirer, M., Duflo, E., Hansen, C., et al. (2016). Double machine learning for treatment and causal parameters. *arXiv preprint arXiv:1608.00060*.

Chernozhukov, V., Chetverikov, D., Demirer, M., Duflo, E., Hansen, C., Newey, W., and Robins, J. (2018). Double/debiased machine learning for treatment and structural parameters. *The Econometrics Journal*, 21(1):C1–C68.

Connors, Alfred F., J., Speroff, T., Dawson, N. V., Thomas, C., Harrell, Frank E., J., Wagner, D., Desbiens, N., Goldman, L., Wu, A. W., Califff, R. M., Fulkerson, William J., J., Vidaillet, H., Broste, S., Bellamy, P., Lynn, J., and Knaus, W. A. (1996). The effectiveness of right heart catheterization in the initial care of critically ill patients. *JAMA*, 276(11):889–897.

Cornfield, J., Haenszel, W., Hammond, E. C., Lilienfeld, A. M., Shimkin, M. B., and Wynder, E. L. (1959). Smoking and lung cancer: Recent evidence and a discussion of some questions. *JNCI: Journal of the National Cancer Institute*, 22(1):173–203.

Crump, R. K., Hotz, V. J., Imbens, G. W., and Mitnik, O. A. (2009). Dealing with limited overlap in estimation of average treatment effects. *Biometrika*, 96(1):187–199.

Dang, L. E., Gruber, S., Lee, H., Dahabreh, I. J., Stuart, E. A., Williamson, B. D., Wyss, R., Díaz, I., Ghosh, D., Kiciman, E., and et al. (2023). A causal roadmap for generating high-quality real-world evidence. *Journal of Clinical and Translational Science*, 7(1):e212.

Díaz, I. and van der Laan, M. J. (2013). Assessing the causal effect of policies: an example using stochastic interventions. *The international journal of biostatistics*, 9(2):161–174.

Díaz, I., Williams, N., Hoffman, K. L., and Schenck, E. J. (2023). Nonparametric causal effects based on longitudinal modified treatment policies. *Journal of the American Statistical Association*, 118(542):846–857.

Fernholz, L. T. (1983). *von Mises Calculus For Statistical Functionals*. Springer New York, New York, NY.

Greifer, N. and Stuart, E. A. (2023). Choosing the causal estimand for propensity score analysis of observational studies.

Gruber, S. and van der Laan, M. J. (2010). A targeted maximum likelihood estimator of a causal effect on a bounded continuous outcome. *The International Journal of Biostatistics*, 6(1).

Györfi, L., Kohler, M., Krzyżak, A., and Walk, H. (2002). *A Distribution-Free Theory of Nonparametric Regression*. Springer-Verlag, New York.

Hernán, M. A. and Robins, J. M. (2020). *Causal Inference: What If*. Chapman & Hall/CRC, Boca Raton.

Hirano, K. and Imbens, G. W. (2001). Estimation of causal effects using propensity score weighting: An application to data on right heart catheterization. *Health Services and Outcomes Research Methodology*, 2(3):259–278.

Imbens, G. W. (2004). Nonparametric estimation of average treatment effects under exogeneity: A review. *The Review of Economics and Statistics*, 86(1):4–29.

Imbens, G. W. and Manski, C. F. (2004). Confidence intervals for partially identified parameters. *Econometrica*, 72(6):1845–1857.

Kang, J. and Schafer, J. (2007). Demystifying double robustness: A comparison of alternative strategies for estimating a population mean from incomplete data (with discussion). *Statistical Science*, 22:523–39.

Karavani, E., Bak, P., and Shimoni, Y. (2019). A discriminative approach for finding and characterizing positivity violations using decision trees.

Kennedy, E. H. (2019). Nonparametric causal effects based on incremental propensity score interventions. *Journal of the American Statistical Association*, 114(526):645–656.

Kennedy, E. H. (2024). Semiparametric doubly robust targeted double machine learning: A review. In *Handbook of Statistical Methods for Precision Medicine*, chapter 10, pages 207–236. Chapman and Hall/CRC, 1 edition.

Kennedy, E. H., Balakrishnan, S., and Wasserman, L. A. (2023). Semiparametric counterfactual density estimation. *Biometrika*, 110(4):875–896.

Lee, B. K., Lessler, J., and Stuart, E. A. (2011). Weight trimming and propensity score weighting. *PLOS ONE*, 6(3):1–6.

Lee, S. and Weidner, M. (2021a). *ATbounds: Bounding Treatment Effects by Limited Information Pooling*. R package version 0.1.0.

Lee, S. and Weidner, M. (2021b). Bounding treatment effects by pooling limited information across observations.

Levis, A. W., Bonvini, M., Zeng, Z., Keele, L., and Kennedy, E. H. (2025). Covariate-assisted bounds on causal effects with instrumental variables. *Journal of the Royal Statistical Society Series B: Statistical Methodology*, page qkaf028.

Li, F., Morgan, K. L., and Zaslavsky, A. M. (2018a). Balancing covariates via propensity score weighting. *Journal of the American Statistical Association*, 113(521):390–400.

Li, F., Thomas, L. E., and Li, F. (2018b). Addressing extreme propensity scores via the overlap weights. *American Journal of Epidemiology*, 188(1):250–257.

Lin, D. Y., Psaty, B. M., and Kronmal, R. A. (1998). Assessing the sensitivity of regression results to unmeasured confounders in observational studies. *Biometrics*, 54(3):948–963.

Ma, X., Sasaki, Y., and Wang, Y. (2024). testing limited overlap. *Econometric Theory*, page 1–34.

Manski, C. F. (1990). Nonparametric bounds on treatment effects. *The American Economic Review*, 80(2):319–323.

Manski, C. F. (1997). Monotone treatment response. *Econometrica*, 65(6):1311–1334.

Manski, C. F. and Pepper, J. V. (2000). Monotone instrumental variables: With an application to the returns to schooling. *Econometrica*, 68(4):997–1010.

McClean, A. and Díaz, I. (2025). Propensity score weighting across counterfactual worlds: longitudinal effects under positivity violations.

Murphy, D. J. and Cluff, L. E. (1990). The SUPPORT study. *Journal of Clinical Epidemiology*, 43:V–X.

Nabi, R., Bonvini, M., Kennedy, E. H., Huang, M.-Y., Smid, M., and Scharfstein, D. O. (2024). Semiparametric sensitivity analysis: unmeasured confounding in observational studies. *Biometrics*, 80(4):ujae106.

Petersen, M. L., Porter, K. E., Gruber, S., Wang, Y., and van der Laan, M. J. (2012). Diagnosing and responding to violations in the positivity assumption. *Statistical Methods in Medical Research*, 21(1):31–54. PMID: 21030422.

Petersen, M. L. and van der Laan, M. J. (2014). Causal models and learning from data: Integrating causal modeling and statistical estimation. *Epidemiology*, 25(3).

Richardson, A., Hudgens, M. G., Gilbert, P. B., and Fine, J. P. (2014). Nonparametric Bounds and Sensitivity Analysis of Treatment Effects. *Statistical Science*, 29(4):596 – 618.

Rizk, J. G. (2025). When and why to use overlap weighting: Clarifying its role, assumptions, and estimand in real-world studies. *Journal of Clinical Epidemiology*, page 111942.

Robins, J. (1989). The analysis of randomized and non-randomized aids treatment trials using a new approach in causal inference in longitudinal studies. In Sechrest, L., Freeman, H., and Mulley, A., editors, *Health Service Methodology: A Focus on AIDS*, pages 113–159. U.S. Public Health Service, National Center for Health Services Research, Washington D.C.

Robins, J., Li, L., Tchetgen Tchetgen, E., and van der Vaart, A. W. (2009). Quadratic semiparametric von mises calculus. *Metrika*, 69(2-3):227–247.

Robins, J., Sued, M., Lei-Gomez, Q., and Rotnitzky, A. (2007). Comment: Performance of double-robust estimators when "inverse probability" weights are highly variable. *Statistical Science*, 22(4):544–559.

Robins, J. M. (1986). A new approach to causal inference in mortality studies with sustained exposure periods - application to control of the healthy worker survivor effect. *Mathematical Modelling*, 7:1393–1512.

Robins, J. M. and Rotnitzky, A. (1995). Semiparametric efficiency in multivariate regression models with missing data. *Journal of the American Statistical Association*, 90(429):122–129.

Rosenbaum, P. R. (2012). Optimal matching of an optimally chosen subset in observational studies. *Journal of Computational and Graphical Statistics*, 21(1):57–71.

Rosenbaum, P. R. and Rubin, D. B. (1983). The central role of the propensity score in observational studies for causal effects. *Biometrika*, 70(1):41–55.

Rothe, C. (2017). robust confidence intervals for average treatment effects under limited overlap. *Econometrica*, 85(2):645–660.

Schlesselman, J. J. (1978). Assessing effects of confounding variables. *American Journal of Epidemiology*, 108(1):3–8.

Schomaker, M., McIlleron, H., Denti, P., and Díaz, I. (2024). Causal inference for continuous multiple time point interventions. *Statistics in Medicine*, 43(28):5380–5400.

Stürmer, T., Rothman, K. J., Avorn, J., and Glynn, R. J. (2010). Treatment effects in the presence of unmeasured confounding: Dealing with observations in the tails of the propensity score distribution—a simulation study. *American Journal of Epidemiology*, 172(7):843–854.

Stürmer, T., Webster-Clark, M., Lund, J. L., Wyss, R., Ellis, A. R., Lunt, M., Rothman, K. J., and Glynn, R. J. (2021). Propensity score weighting and trimming strategies for reducing variance and bias of treatment effect estimates: A simulation study. *American Journal of Epidemiology*, 190(8):1659–1670.

Traskin, M. and Small, D. S. (2011). Defining the study population for an observational study to ensure sufficient overlap: A tree approach. *Statistics in Biosciences*, 3(1):94–118.

Tsiatis, A. A. (2006). *Semiparametric Theory & Missing Data*. Springer.

van der Laan, M. J. and Luedtke, A. R. (2014). Targeted learning of an optimal dynamic treatment, and statistical inference for its mean outcome. Working Paper 317, U.C. Berkeley Division of Biostatistics Working Paper Series.

van der Laan, M. J. and Robins, J. M. (2003). *Unified Methods for Censored Longitudinal Data and Causality*. Springer, New York.

van der Laan, M. J. and Rose, S. (2011). *Targeted Learning: Causal Inference for Observational and Experimental Data*. Springer, New York.

van der Laan, M. J. and Rubin, D. (2006). Targeted maximum likelihood learning. *The International Journal of Biostatistics*, 2(1).

van der Vaart, A. W. (1998). *Asymptotic Statistics*. Cambridge University Press.

van der Vaart, A. W. and Wellner, J. A. (1996). *Weak Convergence and Empirical Processes*. Springer-Verlag New York.

VanderWeele, T. J. and Arah, O. A. (2011). Bias formulas for sensitivity analysis of unmeasured confounding for general outcomes, treatments, and confounders. *Epidemiology*, 22(1):42–52.

Visconti, G. and Zubizarreta, J. R. (2018). Handling limited overlap in observational studies with cardinality matching. *Observational Studies*, 4(1):217–249.

von Mises, R. (1947). On the asymptotic distribution of differentiable statistical functions. *The annals of mathematical statistics*, 18(3):309–348.

Whitehouse, J., Austern, M., and Syrgkanis, V. (2025). Inference on optimal policy values and other irregular functionals via smoothing.

Wolf, G., Shabat, G., and Shteingart, H. (2021). Positivity validation detection and explainability via zero fraction multi-hypothesis testing and asymmetrically pruned decision trees.

Zheng, W. and van der Laan, M. J. (2011). Cross-validated targeted minimum-loss-based estimation. In *Targeted Learning*, pages 459–474. Springer.

Zhou, Y., Matsouaka, R. A., and Thomas, L. (2020). Propensity score weighting under limited overlap and model misspecification. *Statistical Methods in Medical Research*, 29(12):3721–3756. PMID: 32693715.

Zhu, Y., Hubbard, R. A., Chubak, J., Roy, J., and Mitra, N. (2021). Core concepts in pharmacoepidemiology: Violations of the positivity assumption in the causal analysis of observational data: Consequences and statistical approaches. *Pharmacoepidemiology and Drug Safety*, 30(11):1471–1485.

Zivich, P. N., Edwards, J. K., Lofgren, E. T., Cole, S. R., Shook-Sa, B. E., and Lessler, J. (2024a). Transportability without positivity: A synthesis of statistical and simulation modeling. *Epidemiology*, 35(1).

Zivich, P. N., Edwards, J. K., Shook-Sa, B. E., Lofgren, E. T., Lessler, J., and Cole, S. R. (2024b). Synthesis estimators for transportability with positivity violations by a continuous covariate. *Journal of the Royal Statistical Society Series A: Statistics in Society*, 188(1):158–180.

A Results for Section 3.1

A.1 Derivations of efficient influence functions

The following lemmas derive the efficient influence functions of the parameters $\psi(c)$, L_s , and U_s . The proofs follow a similar structure. First, we use heuristic techniques to derive putative EIFs;

in particular, we draw on several “tricks” from Kennedy (2024), which we refer to for further explanation. We then show that the parameter satisfies the von-Mises expansion (6) by deriving the form of the second-order remainder term. By showing that the remainder term is second-order, and that the putative EIF is bounded, an appeal to (Kennedy et al., 2023, Lemma 2) establishes that the putative EIF is the EIF.

Lemma 1 (Efficient influence function of $\psi_s(c)$). *Fix $c \in [0, \frac{1}{2}]$. The parameter $\psi_s(c)$ is pathwise differentiable with uncentered efficient influence function given by*

$$\begin{aligned}\varphi_{\psi_s}(Z) = & \frac{A}{\pi} s_g(\pi, c, \gamma) \{Y - \mu_1\} - \frac{1 - A}{1 - \pi} s_l(\pi, 1 - c, \gamma) \{Y - \mu_0\} \\ & + \{\mu_1 \dot{s}_g(\pi, c, \gamma) - \mu_0 \dot{s}_l(\pi, 1 - c, \gamma)\} \{A - \pi\} \\ & + \mu_1 s_g(\pi, c, \gamma) - \mu_0 s_l(\pi, 1 - c, \gamma).\end{aligned}$$

Proof. Write $\psi(c) = \psi_1(c) - \psi_2(c)$, with $\psi_1(c) = \mathbb{E} \{\mu_1(X) s_g(\pi(X), c, \gamma)\}$ and $\psi_2(c) = \mathbb{E} \{\mu_0(X) s_l(\pi(X), 1 - c, \gamma)\}$. We derive the EIF φ_{ψ_1} of $\psi_1(c)$; the EIF φ_{ψ_2} of $\psi_2(c)$ follows from similar arguments. The EIF of $\psi(c)$ is then simply $\varphi_{\psi} = \varphi_{\psi_1} - \varphi_{\psi_2}$.

We begin by proposing a putative EIF of ψ_1 :

$$\begin{aligned}\mathbb{IF}(\psi_1(c)) = & \mathbb{IF} \left\{ \sum_x \mu_1(x) s_g(\pi(x), c, \gamma) p(x) \right\} \quad (\text{Trick 1}) \\ = & \sum_x \mathbb{IF} \{\mu_1(x)\} s_g(\pi(x), c, \gamma) p(x) \quad (\text{Trick 2a}) \\ & + \mu_1(x) \mathbb{IF} \{s_g(\pi(x), c, \gamma)\} p(x) \\ & + \mu_1(x) s_g(\pi(x), c, \gamma) \mathbb{IF} \{p(x)\} \\ = & \sum_x \frac{\mathbb{I}(X = x, A = 1)}{p(1, x)} (Y - \mu_1(x)) s_g(\pi(x), c, \gamma) p(x) \quad (\text{Trick 3}) \\ & + \mu_1(x) \dot{s}_g(\pi(x), c, \gamma) \frac{\mathbb{I}[X = x]}{p(x)} (A - \pi(x)) p(x) \quad (\text{Trick 2b and Trick 3}) \\ & + \mu_1(x) s_g(\pi(x), c, \gamma) (\mathbb{I}(X = x) - p(x)) \\ = & \frac{A}{\pi(X)} s_g(\pi(X), c, \gamma) (Y - \mu_1(X)) \\ & + \mu_1(X) \dot{s}_g(\pi(X), c, \gamma) (A - \pi(X)) \\ & + \mu_1(X) s_g(\pi(X), c, \gamma) - \psi_1(c).\end{aligned}$$

Next, we derive the second-order remainder for ψ_1 induced by the putative EIF. Let $\mathbb{P}, \hat{\mathbb{P}} \in \mathcal{P}$. We denote expectations, nuisance parameters, and the EIF of the parameter with respect to $\hat{\mathbb{P}}$ as $\hat{\mathbb{E}}$, $\hat{\mu}$, $\hat{\pi}$, and $\hat{\varphi}$, respectively. We will also write $s(\pi) \equiv s_g(\pi, c, \gamma)$. Arguments are suppressed throughout.

$$\begin{aligned}\mathbb{R}_{\psi_1}(\mathbb{P}, \hat{\mathbb{P}}) = & -\hat{\mathbb{E}} \{\varphi_{\psi_1}(Z)\} + \hat{\psi} \\ = & -\hat{\mathbb{E}} \left\{ \frac{A}{\pi} s(\pi) (Y - \mu) + \mu \dot{s}(\pi) (\hat{\pi} - \pi) + \mu s(\pi) \right\} + \hat{\mathbb{E}} \{\hat{\mu} s(\hat{\pi})\} \\ = & \hat{\mathbb{E}} \left\{ -s(\pi) \frac{\hat{\pi}}{\pi} (\hat{\mu} - \mu) - \mu \dot{s}(\pi) (\hat{\pi} - \pi) - \mu s(\pi) + \hat{\mu} s(\hat{\pi}) \right\} \\ = & \hat{\mathbb{E}} \left\{ \frac{s(\pi)}{\pi} (\pi - \hat{\pi}) (\hat{\mu} - \mu) - \mu \dot{s}(\pi) (\hat{\pi} - \pi) + \hat{\mu} s(\hat{\pi}) - \hat{\mu} s(\pi) \right\}\end{aligned}$$

Applying a second-order Taylor expansion of $\hat{\mu}s(\pi)$ around $s(\hat{\pi})$, the latter three terms inside the expectation simplify:

$$\begin{aligned} -\mu\dot{s}(\pi)(\hat{\pi} - \pi) + \hat{\mu}s(\hat{\pi}) - \hat{\mu}s(\pi) &= -\mu\dot{s}(\pi)(\hat{\pi} - \pi) - \hat{\mu}\dot{s}(\hat{\pi})(\pi - \hat{\pi}) - \frac{1}{2}\hat{\mu}\ddot{s}(\hat{\pi})(\pi - \hat{\pi})^2 + o\left((\pi - \hat{\pi})^2\right) \\ &= (\hat{\mu}\dot{s}(\hat{\pi}) - \mu\dot{s}(\pi))(\hat{\pi} - \pi) - \frac{1}{2}\hat{\mu}\ddot{s}(\hat{\pi})(\pi - \hat{\pi})^2 + o\left((\pi - \hat{\pi})^2\right), \end{aligned}$$

where \ddot{s} is the second derivative of $x \mapsto s(x)$. Therefore

$$R_{\psi_1}(\mathbb{P}, \hat{\mathbb{P}}) = \hat{\mathbb{E}} \left\{ \frac{s(\pi)}{\pi} (\pi - \hat{\pi}) (\hat{\mu} - \mu) + (\hat{\mu}\dot{s}(\hat{\pi}) - \mu\dot{s}(\pi))(\hat{\pi} - \pi) - \frac{1}{2}\hat{\mu}\ddot{s}(\hat{\pi})(\pi - \hat{\pi})^2 + o\left((\pi - \hat{\pi})^2\right) \right\}.$$

The remainder term R_{ψ_1} is indeed second-order, depending only on products squares of differences in the nuisance parameters. Finally, we argue that the variance of the EIF is bounded. This follows from the fact that outcome is bounded, the smooth approximation function s_ψ is bounded, and the derivative of the smooth approximation is bounded by definition. Therefore by (Kennedy et al., 2023, Lemma 2), φ_{ψ_1} is the EIF of ψ_1 . \square

Lemma 2 (Efficient influence function of $L_s(c)$). *Fix $c \in [0, \frac{1}{2}]$. The parameter $L_s(c)$ is pathwise differentiable with uncentered efficient influence function given by*

$$\varphi_{L_s}(Z) = \varphi_{\psi_s}(Z) - \dot{s}_g(\pi, c, \gamma) \{A - \pi\} - s_g(\pi, c, \gamma).$$

Proof. The proof follows a similar structure as the proof of Lemma 1, and we adopt the same notational conveniences. Within only this proof, let $\theta(c) = \mathbb{E}\{s_g(\pi, c, \gamma)\}$, so that $L_s(c) = \psi_s(c) + [1 - \theta(c)]$. We derive the EIF of $\theta(c)$, from which the EIF for $L_s(c)$ follows by combining with the EIF of $\psi_s(c)$ (Lemma 1). For convenience we may write $s(\pi) \equiv s_g(\pi > c)$. A putative EIF of $\theta(c)$ is

$$\begin{aligned} \mathbb{IF}(\theta(c)) &= \mathbb{IF} \left\{ \sum_x s(\pi(x) > c) p(x) \right\} && \text{Trick 1} \\ &= \sum_x \mathbb{IF}\{s(\pi(x) > c)\} p(x) + s(\pi(x) > c) \mathbb{IF}\{p(x)\} && \text{Trick 2a} \\ &= \sum_x \dot{s}_g(\pi(x), c, \gamma) \frac{\mathbb{I}(X = x)}{p(x)} (A - \pi(x)) p(x) + s(\pi(x) > c) (\mathbb{I}(X = x) - p(x)) \\ &= \dot{s}_g(\pi(X), c, \gamma) (A - \pi(X)) + s_g(\pi(X), c, \gamma) - \theta(c). \end{aligned}$$

The second-order term is

$$\begin{aligned} R_\theta(\mathbb{P}, \hat{\mathbb{P}}) &= -\hat{\mathbb{E}}\{\varphi_\theta(Z)\} + \hat{\theta} \\ &= -\hat{\mathbb{E}}\{\dot{s}(\pi)(A - \pi) + s(\pi)\} + \hat{\mathbb{E}}\{s(\hat{\pi})\} \\ &= \hat{\mathbb{E}}\{-\dot{s}(\pi)(\hat{\pi} - \pi) - s(\pi) + s(\hat{\pi})\} \end{aligned}$$

Expanding $s(\pi)$ about $s(\hat{\pi})$ yields:

$$\begin{aligned} &= \hat{\mathbb{E}} \left\{ -\dot{s}(\pi)(\hat{\pi} - \pi) + \dot{s}(\hat{\pi})(\hat{\pi} - \pi) - \frac{1}{2}\ddot{s}(\hat{\pi})(\pi - \hat{\pi})^2 - o\left((\hat{\pi} - \pi)^2\right) \right\} \\ &= \hat{\mathbb{E}} \left\{ (\dot{s}(\hat{\pi}) - \dot{s}(\pi))(\hat{\pi} - \pi) - \frac{1}{2}\ddot{s}(\hat{\pi})(\pi - \hat{\pi})^2 - o\left((\hat{\pi} - \pi)^2\right) \right\}. \end{aligned}$$

This shows that the remainder term is indeed second-order. The variance of φ_θ is bounded, as both s and \dot{s} are bounded by construction. Therefore φ_θ is the EIF of $\theta(c)$ by Kennedy et al. 2023, Lemma 2. The EIF of L_s follows by combining EIFs for $\psi(c)$ and $\theta(c)$. \square

Lemma 3 (Efficient influence function of $U_s(c)$). *Fix $c \in [0, \frac{1}{2}]$. The parameter $U_s(c)$ is pathwise differentiable with uncentered efficient influence function given by*

$$\varphi_{U_s}(Z) = \varphi_{\psi_s}(Z) + \dot{s}(\pi < 1 - c) \{A - \pi\} + s_l(\pi, 1 - c, \gamma).$$

Proof. The proof follows from minor modifications to the proof of Lemma 2. \square

A.2 Proof of Theorem 1

The proof follows from Lemmas 1, 2, and 3

A.3 Proof of Theorem 2

The weak convergence of TMLE estimators based on cross-fitted nuisance estimators is well-established; see for example (Díaz et al., 2023, Theorem 3) and its proof, which can be easily adapted to this setting. The key steps are first to see that, by construction of the fluctuation models and the choice of loss function, the fluctuated estimates $\hat{\eta}^*$ solve the empirical EIF estimating equation, implying null first-order bias of the associated debiased plug-in estimators. Second, the use of cross-fitting for the nuisance estimators allows control of the empirical process remainder term.

A.4 Proof of Theorem 3

Proof. For this proof we use the same notation as in Algorithm 2.

Joint weak convergence:

By Theorem 2, the estimators satisfy a joint linear expansion; i.e.,

$$\sqrt{n} \begin{pmatrix} \hat{L}_1 - L_1 \\ \vdots \\ \hat{L}_K - L_K \\ \hat{U}_1 - U_1 \\ \vdots \\ \hat{U}_K - U_K \end{pmatrix} = n^{-1/2} \sum_{i=1}^n \begin{pmatrix} \varphi_{L,1}(Z_i, \eta) - L_1 \\ \vdots \\ \varphi_{L,K}(Z_i, \eta) - L_K \\ \varphi_{U,1}(Z_i, \eta) - U_1 \\ \vdots \\ \varphi_{U,K}(Z_i, \eta) - U_K \end{pmatrix} + \begin{pmatrix} o_{\mathbb{P}}(1) \\ \vdots \\ o_{\mathbb{P}}(1) \end{pmatrix}.$$

The multivariate CLT yields joint weak convergence to a multivariate Gaussian with covariance matrix $\mathbb{E}\{\varphi(Z)\varphi(Z)^T\}$ where

$$\varphi(Z) = \left(\varphi_{L,1}(Z_i, \eta) - L_1, \dots, \varphi_{L,K}(Z_i, \eta) - L_K, \varphi_{U,1}(Z_i, \eta) - U_1, \dots, \varphi_{U,K}(Z_i, \eta) - U_K \right)^T.$$

Remark 3. From here, one could use the multivariate Gaussian limit to conduct inference by sampling from $N(0, \mathbb{E}(\varphi\varphi^T))$. We instead use the multiplier bootstrap.

Event equivalence:

Let $T_{L,k} = \sqrt{n} \left(\frac{\hat{L}_k - L_k}{\hat{\sigma}_{L,k}} \right)$ and $T_{U,k} = \sqrt{n} \left(\frac{U_k - \hat{U}_k}{\hat{\sigma}_{U,k}} \right)$. For any fixed $t \geq 0$ and each k ,

$$L_k \geq \hat{L}_k - t \frac{\hat{\sigma}_{L,k}}{\sqrt{n}} \iff T_{L,k} \leq t, \quad U_k \leq \hat{U}_k + t \frac{\hat{\sigma}_{U,k}}{\sqrt{n}} \iff T_{U,k} \leq t.$$

The inequalities on the left-hand side of each equivalence are reversed because $T_{L,k}$ and $T_{U,k}$ are reversed. Next, notice that the following two events are equivalent:

$$\left\{ \forall k : L_k \geq \widehat{L}_k - t \frac{\widehat{\sigma}_{L,k}}{\sqrt{n}} \text{ and } U_k \leq \widehat{U}_k + t \frac{\widehat{\sigma}_{U,k}}{\sqrt{n}} \right\}$$

and

$$\left\{ \max_k \max\{T_{L,k}, T_{U,k}\} \leq t \right\}.$$

Moreover, notice both events also imply a third event. Let $k_L = \operatorname{argmax}_k \widehat{L}_k - t \widehat{\sigma}_{L,k} / \sqrt{n}$ and $k_U = \operatorname{argmin}_k \widehat{U}_k + t \widehat{\sigma}_{U,k} / \sqrt{n}$. Then, both events above imply

$$\left\{ L_{k_L} \geq \max_k \widehat{L}_k - t \frac{\widehat{\sigma}_{L,k}}{\sqrt{n}}, U_{k_U} \leq \min_k \widehat{U}_k + t \frac{\widehat{\sigma}_{U,k}}{\sqrt{n}} \right\},$$

By Proposition 2, $\mathbb{E}(Y^1 - Y^0) \in [L_k, U_k]$ for every k ; indeed, $\mathbb{E}(Y^1 - Y^0) \in [L_j, U_k]$ for every k, j . Therefore, the previous event implies

$$\left\{ \mathbb{E}(Y^1 - Y^0) \in \left[\max_k \widehat{L}_k - t \frac{\widehat{\sigma}_{L,k}}{\sqrt{n}}, \min_k \widehat{U}_k + t \frac{\widehat{\sigma}_{U,k}}{\sqrt{n}} \right] \right\},$$

Therefore,

$$\begin{aligned} \mathbb{P} \left\{ \max_k \max\{T_{L,k}, T_{U,k}\} \leq t \right\} &\leq \mathbb{P} \left\{ \forall k : \mathbb{E}(Y^1 - Y^0) \in \left[\widehat{L}_k - t \frac{\widehat{\sigma}_{L,k}}{\sqrt{n}}, \widehat{U}_k + t \frac{\widehat{\sigma}_{U,k}}{\sqrt{n}} \right] \right\} \text{ and} \\ \mathbb{P} \left\{ \max_k \max\{T_{L,k}, T_{U,k}\} \leq t \right\} &\leq \mathbb{P} \left\{ \mathbb{E}(Y^1 - Y^0) \in \left[\max_k \widehat{L}_k - t \frac{\widehat{\sigma}_{L,k}}{\sqrt{n}}, \min_k \widehat{U}_k + t \frac{\widehat{\sigma}_{U,k}}{\sqrt{n}} \right] \right\} \end{aligned}$$

and so a lower bound on the left-hand probability implies a lower bound on the right-hand probabilities.

Multiplier bootstrap approximation:

Let $\widehat{M} := \max_k \max\{T_{L,k}, T_{U,k}\}$. Using the notation from above, the left-hand probability is $\mathbb{P}(\widehat{M} \leq t)$. We want to show $\mathbb{P}(\widehat{M} \leq \widehat{q}_{1-\alpha}) \geq 1 - \alpha + o_{\mathbb{P}}(1)$.

By the joint weak convergence result above and the continuous mapping theorem for the max map, $\widehat{M} \rightsquigarrow M$. Hence,

$$\sup_{t \in \mathbb{R}} \left| \mathbb{P}(\widehat{M} \leq t) - \mathbb{P}(M \leq t) \right| = o(1).$$

Meanwhile, by standard analysis of the multiplier bootstrap and the continuity of the max-max transformation with a fixed set of thresholds (van der Vaart and Wellner, 1996, Theorem 2.9.6),

$$\sup_{t \in \mathbb{R}} \left| \mathbb{P}(\widehat{M}^{(b)} \leq t \mid \mathbf{Z}_n) - \mathbb{P}(\widehat{M} \leq t) \right| = o_{\mathbb{P}}(1),$$

where \mathbf{Z}_n denotes the data, so the first probability is conditional on the data.

Next, let $\widetilde{q}_{1-\alpha}$ denote the exact bootstrap $1 - \alpha$ quantile, so that $\mathbb{P}(\widehat{M}^{(b)} \leq \widetilde{q}_{1-\alpha} \mid \mathbf{Z}_n) = 1 - \alpha$. By the previous display,

$$\mathbb{P}(\widehat{M} \leq \widetilde{q}_{1-\alpha}) = 1 - \alpha + o_{\mathbb{P}}(1).$$

Finally, we address the Monte Carlo error. Assuming $B \rightarrow \infty$ as $n \rightarrow \infty$,

$$\widehat{q}_{1-\alpha} \xrightarrow{P} \widetilde{q}_{1-\alpha}.$$

N	γ	95% UI Width									
		Mean				Median		90% Quantile		Std. Dev.	
		Bounds	DR	Bounds	DR	Bounds	DR	Bounds	DR	Bounds	DR
100	10^{-3}	0.47	0.81	0.45	0.47	0.56	2.00	0.07	0.64		
	10^{-2}	0.47	0.81	0.45	0.47	0.56	2.00	0.07	0.64		
	10^{-1}	0.46	0.81	0.45	0.47	0.54	2.00	0.06	0.64		
250	10^{-3}	0.28	0.29	0.27	0.26	0.32	0.30	0.03	0.19		
	10^{-2}	0.28	0.29	0.27	0.26	0.32	0.30	0.03	0.19		
	10^{-1}	0.28	0.29	0.27	0.26	0.32	0.30	0.03	0.19		
500	10^{-3}	0.19	0.18	0.19	0.18	0.21	0.19	0.02	0.01		
	10^{-2}	0.19	0.18	0.19	0.18	0.21	0.19	0.02	0.01		
	10^{-1}	0.19	0.18	0.19	0.18	0.21	0.19	0.02	0.01		
1000	10^{-3}	0.13	0.13	0.13	0.13	0.14	0.13	0.01	0.00		
	10^{-2}	0.13	0.13	0.13	0.13	0.14	0.13	0.01	0.00		
	10^{-1}	0.13	0.13	0.13	0.13	0.14	0.13	0.01	0.00		

Table 3: Empirical coverage and power results from Simulation Study 1 (Section 5) for simulations generated unconditionally from the simulation DGP with overlap parameter $\alpha = 1$. Results compare the 95% uncertainty intervals of a doubly-robust one-step estimator (DR) and the tightest uniform 95% non-overlap bounds (Bounds) across a grid of propensity score thresholds and smoothness parameters in terms of the mean, median, 90%, quantile, and standard deviation of the uncertainty interval width.

Therefore,

$$\mathbb{P} \left(\widehat{M} \leq \widehat{q}_{1-\alpha} \right) = 1 - \alpha + o_{\mathbb{P}}(1).$$

The results follow from the definition of \widehat{M} and the event equivalence argument above. \square

B Additional simulation results

Tables 3 and 4 mirror Tables 1 and 2, from the main text, but with the simulation DGP overlap parameter $\alpha = 1$ rather than $\alpha = 5$. These results therefore illustrate the performance of the non-overlap bounds in a setting without extreme positivity violations. In this setting, both the non-overlap bounds and the doubly-robust one-step estimator exhibit somewhat better performance at small sample sizes, but as sample size increases the two methods have similar performance in terms of uncertainty interval width, empirical coverage, and power as sample size increases.

N	γ	95% Coverage		Power	
		Bounds	DR	Bounds	DR
100	10^{-3}	96.4%	96.4%	0.47	0.38
	10^{-2}	96.3%	96.4%	0.47	0.38
	10^{-1}	96.5%	96.4%	NA	0.38
250	10^{-3}	96.0%	95.3%	0.90	0.89
	10^{-2}	96.0%	95.3%	0.91	0.89
	10^{-1}	95.9%	95.3%	0.93	0.89
500	10^{-3}	96.2%	95.3%	1.00	1.00
	10^{-2}	96.2%	95.3%	1.00	1.00
	10^{-1}	96.5%	95.3%	1.00	1.00
1000	10^{-3}	96.0%	95.0%	1.00	1.00
	10^{-2}	96.0%	95.0%	1.00	1.00
	10^{-1}	95.3%	95.0%	1.00	1.00

Table 4: Empirical coverage and power results from Simulation Study 1 (Section 5) for simulations generated unconditionally from the simulation DGP with overlap parameter $\alpha = 1$. Results compare the 95% uncertainty intervals of a doubly-robust one-step estimator (DR) and the tightest uniform 95% non-overlap bounds (Bounds) across a grid of propensity score thresholds and smoothness parameters in terms of empirical 95% coverage and power.

C Replication R code for application

The code listing below reproduces the results from the application (Section 6). Figure 3 shows the non-overlap bounds from the data application with the alternative smoothness parameter $\gamma = 0.001$.

```
# Install ATbounds package for data:
# install.packages("ATbounds")
#
# Install effectbounds package:
# remotes::install_github("herbps10/effectbounds")

library(effectbounds)

set.seed(10016)

data("RHC", package = "ATbounds")

X <- setdiff(colnames(RHC), c("survival", "RHC"))
A <- "RHC"
Y <- "survival"

thresholds <- 10^seq(-5, log10(0.05), 0.2)
smoothness <- c(0.001, 0.01)

bounds <- ate_bounds(
  RHC, X, A, Y,
  smoothness = smoothness,
  thresholds = thresholds
)

summary(bounds)

title <- "Population Average Treatment Effect of \nRight Heart Catheterization on
30-day Mortality"
ylim = c(-0.2, 0.10)

pdf("application/rhc_plot.pdf", width = 8, height = 6)
plot(bounds,
      main = title,
      ylim = ylim,
      bounds_color = "darkred", smoothness = 0.01)
dev.off()

pdf("application/rhc_plot_sensitivity.pdf", width = 8, height = 6)
plot(bounds,
      main = title,
      ylim = ylim,
      bounds_color = "darkred", smoothness = 0.001)
dev.off()
```

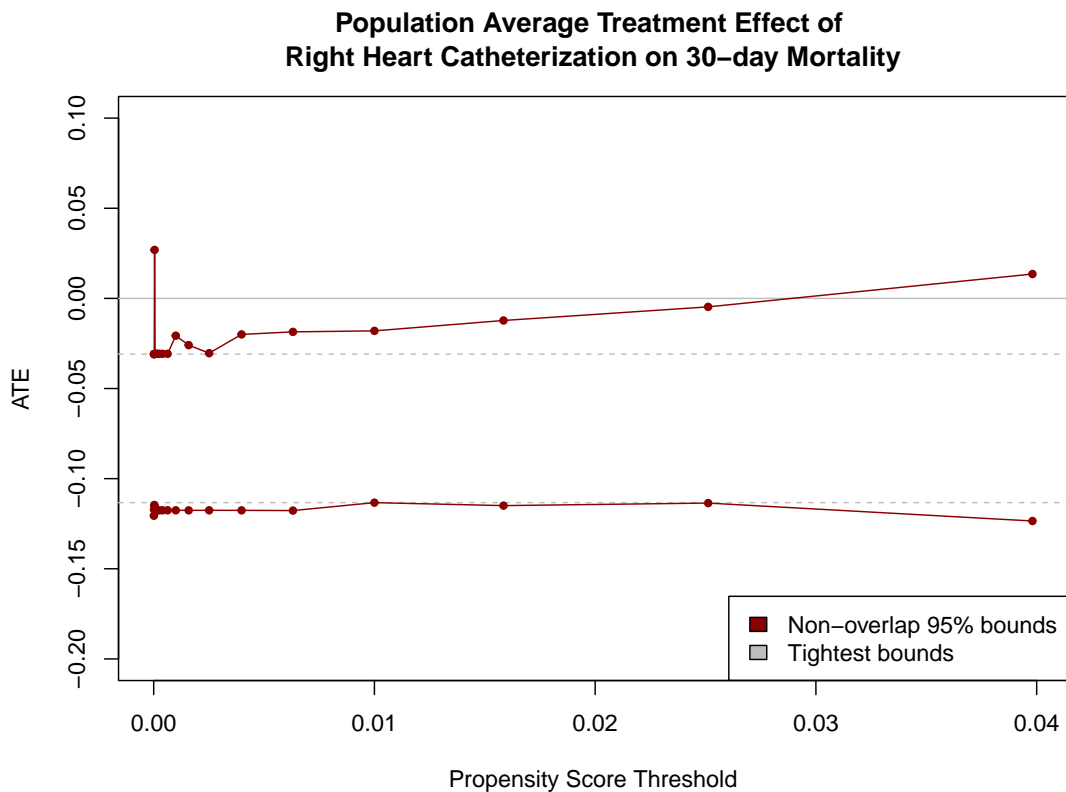


Figure 3: Uniform 95% non-overlap bounds (for $\gamma = 0.001$) on the average treatment effect (ATE) of right heart catheterization on survival. The points illustrate the lower and upper bounds with respect to a logarithmic grid of propensity score thresholds. The lines between points are solely to guide the eye. The horizontal dotted lines indicate the tightest valid 95% uncertainty interval that may be formed from the non-overlap bounds.